JOURNAL OF GEOPHYSICAL RESEARCH, VOL. 100, NO. C12, PAGES 25,109–25,127, DECEMBER 15, 1995

Open-ocean validation of TOPEX/POSEIDON sea level in the western equatorial Pacific

Joël Picaut,[1] Antonio J. Busalacchi,[2] Michael J. McPhaden,[3] Lionel Gourdeau,[1] Frank I. Gonzalez,[3] and Eric C. Hackert[2,4]

Abstract. During the verification phase of the TOPEX/POSEIDON radar altimeter mission a rigorous open-ocean validation experiment was conducted in the western equatorial Pacific Ocean. From August–September 1992 to February–March 1993, two Tropical Ocean and Global Atmosphere (TOGA) Tropical Atmosphere Ocean moorings at 2°S-156°E (1739 m depth) and 2°S-164.4°E (4400 m depth) were outfitted with additional temperature, salinity, and pressure sensors to measure precisely the dynamic height from the surface to the bottom at 5-min intervals directly beneath two TOPEX/POSEIDON crossovers. Bottom pressure gauges and inverted echo sounders were deployed as well. A predeployment design study using full depth conductivity-temperature-depth casts, subsequently confirmed by postdeployment analyses, indicated this suite of instruments was capable of measuring sea surface height fluctuations to within 1–2 cm. The validation experiment also benefited from the comprehensive set of ocean-atmosphere measurements that were made in the region during the TOGA Coupled Ocean-Atmosphere Response Experiment intensive observation period of November 1992 to February 1993. The surface relative to bottom dynamic height fluctuations observed in situ during the 6–7 month experiment had a standard deviation of 5 cm with excursions of order ±15 cm. Energetic steric sea level variability was found to exist on short timescales of order hours to a few days, most notably, the quasi-permanence of strong semidiurnal internal tides. Such internal tides were noted to induce changes in surface dynamic height with a standard deviation of 2 dynamic centimeters. At the shallower of the two sites, 2°S-156°E, a possible nonlinear rectification of the internal tide was observed occasionally to change the dynamic height by as much as 30 cm over less than an hour. On timescales longer than the 10-day repeat of the TOPEX/POSEIDON satellite, the low-frequency fluctuations of dynamic height were related to interannual variations corresponding to the 1991–1993 El Niño–Southern Oscillation, to the seasonal cycle, and to intraseasonal variations associated with the 40- to 60-day oscillations of the equatorial zonal wind field. Instantaneous comparisons between the 1-s TOPEX/POSEIDON altimeter retrievals and the 5-min dynamic height were performed with regard to several tide models, the barotropic tide measured in situ, European Centre for Medium-Range Weather Forecasts surface air pressure, and the surface air pressure measured in situ. Depending on the choice of altimeter and of the environmental corrections applied to the altimeter data, the rms differences between the satellite and the in situ measurements of sea level were as low as 3.3 cm at 2°S-156°E and 3.7 cm at 2°S-164.4°E. When additional satellite data in the general vicinity of the mooring are included and after the use of a 30-day low-pass filter, the satellite and in situ data were found to be highly correlated, with correlation coefficients of about 0.95 and rms differences around 1.8 cm.

1. Introduction

The initial results from the TOPEX/POSEIDON radar altimeter mission are very encouraging with respect to the capability of the altimeter to describe the sea level attributes of the large-scale ocean circulation (see the special section "TOPEX/POSEIDON: Geophysical Evaluation" in *Journal of Geophysical Research*, *99*(C12), 24,369–25,062, 1994). Prior to launch, the precision of the radar altimeter instrument was projected to be of order 2.4 cm [*TOPEX/POSEIDON Science Working Team*, 1991]. In the event this level of precision is attained in orbit and the necessary environmental corrections are of similar order and result in an overall level of accuracy of order 4 cm, this class of radar altimeters will have considerable potential for long-term ocean climate monitoring. Thus there is a clear need to rigorously validate the accuracy of TOPEX/POSEIDON sea level observations in the open ocean. Unfortunately, an open-ocean validation was not planned by the TOPEX/POSEIDON project. During the verification phase of

[1]Groupe SURTROPAC, l'Institut Français de Recherche Scientifique pour le Développement en Coopération (ORSTOM), Nouméa, New Caledonia.
[2]Laboratory for Hydrospheric Processes, NASA Goddard Space Flight Center, Greenbelt, Maryland.
[3]Pacific Marine Environmental Laboratory, NOAA, Seattle, Washington.
[4]Hughes STX Corporation, Greenbelt, Maryland.

Paper number 95JC021
0148-0227/95/95JC-021

the mission the project sponsored calibration and validation experiments at Harvest Platform in the coastal waters off California and on the island of Lampedusa near Sicily [*TOPEX/POSEIDON Joint Verification Team*, 1992]. These efforts were directed more toward validating the altimeter range delay between the satellite and the sea surface than with characterizing the TOPEX/POSEIDON accuracy when monitoring open-ocean sea level variability.

Any attempt to validate TOPEX/POSEIDON in the open ocean is complicated by the fact that the intrinsic error of most in situ sea level estimates is of order 3 to 7 cm. The range of these errors depends on the particular measurement technique and its inherent limitations. For example, sea level deduced from island tide gauges is contaminated by interactions between the island and local currents, shelf effects, and wind setup. Dynamic height time series obtained from moorings, ship of opportunity expendable bathythermographs (XBT), conductivity-temperature-depth (CTD) casts, and inverted echo sounders (IES) are used to estimate the steric sea level contribution. The significance of the sea level estimated from these instruments and platforms is constrained by technical issues such as the reference level, the use of a mean temperature-salinity relation, and inadequate space-time sampling. Therefore there is a fundamental difference between the anticipated TOPEX/POSEIDON accuracy and any present observational means for in situ validation.

Here we present the results from a field experiment that was carefully designed for the expressed purpose of using in situ observations to validate open-ocean TOPEX/POSEIDON altimeter retrievals in the western equatorial Pacific during the 6-month verification phase. The validation of TOPEX/POSEIDON sea level in the equatorial Pacific Ocean is of particular interest because of the important climatic impact of changes in the tropical Pacific Ocean circulation related to the El Niño–Southern Oscillation (ENSO) phenomenon. Although the Geosat altimeter was capable of resolving the order 20-cm changes in sea level associated with the 1986–1987 El Niño [*Miller et al.*, 1988], considerably better accuracy is required to detect significant attributes of the seasonal and interannual variability of the tropical Pacific Ocean. The order 2- to 4-cm accuracy expected from TOPEX/POSEIDON is required if there is to be any hope of monitoring the tropical Pacific seasonal cycle of sea level (of order 5 cm standard deviation [*McPhaden et al.*, 1988]), quantifying the variability of low-latitude surface currents [*Picaut et al.*, 1990], diagnosing western boundary wave reflections thought to be important in ENSO mechanisms such as the delayed action oscillator [*Boulanger and Menkes*, this issue], or initializing ENSO prediction models [*Fischer et al.*, 1994].

The platforms used for this validation experiment consisted of two ATLAS moorings of the Tropical Ocean and Global Atmosphere–Tropical Atmosphere Ocean (TOGA-TAO) array [*Hayes et al.*, 1991]. The TAO array was implemented as part of the 10-year TOGA program for studies of seasonal to interannual climate variability, the most prominent mode of which is the ENSO phenomenon. TOGA-TAO has expanded from a few sites at the start of TOGA in 1985 to an array that presently consists of approximately 70 moorings spanning the tropical Pacific between 8°N and 8°S, 95°W to 137°E [*McPhaden*, 1993].

The two validation moorings used in this study were specifically situated directly beneath TOPEX/POSEIDON crossovers at 2°S-156°E and 2°S-164.4°E (Figure 1). On these two moorings, additional dedicated sensors were deployed (August–September 1992 to February–March 1993) based on a design study estimated to yield sea level with a 1- to 2-cm accuracy. Temperature and salinity sensors were added to the mooring line, from the surface to the bottom, to estimate the steric part of changes in sea level. Inverted echo sounders were deployed as independent measures of the steric variability. Bottom pressure sensors were deployed to determine the barotropic component, and atmospheric pressure sensors were deployed to account for the inverse barometric effect.

The site for this validation experiment was based on the availability of additional in situ measurements in the region. Historical hydrographic information exists around the 2°S-164.4°E site because numerous cruise data (mostly from the French Surveillance Tropical Pacifique (SURTROPAC) program and the U.S./People's Republic of China bilateral program) and ATLAS mooring data have been collected there since 1985. The hydrographic data collected at this site were used to evaluate Geosat in 1986–1987 [*Delcroix et al.*, 1991] and to design the vertical array of sensors used in this experiment. The 2°S-156°E ATLAS mooring, installed in September 1992, has the advantage of being located at the center of the TOGA Coupled Ocean-Atmosphere Response Experiment (COARE) intensive flux array. This array provided unprecedented ocean-atmosphere measurements (e.g., temperature, salinity, currents, turbulence, wind, rain, pressure, humidity, radiation) during the experiment's intensive observation period (November 1992 to February 1993) and was designed to study the interactions between the ocean and the atmosphere within the western Pacific warm pool region [*Webster and Lukas*, 1992]. The suite of observations from ships, moorings, drifters, islands, aircraft, and satellites provides a tremendous opportunity to place the point measurements of sea level at the TOPEX/POSEIDON crossovers in a larger regional context. Lastly, the two mooring sites were located in very different geographical settings. The 2°S-164.4°E mooring was anchored on an abyssal plain (4400 m) far from a coast, whereas the 2°S-156°E mooring was situated on the Ontong Java Plateau (1750 m) near the Kilinailau trench and a little more than a first baroclinic mode radius of deformation (400 km) from New Ireland and Bougainville islands. The sea level comparisons between these two sites permit the quality of the TOPEX/POSEIDON retrievals to be interpreted with regard to the barotropic and baroclinic variability of two different depth regimes.

The present study complements a number of related studies of TOPEX/POSEIDON observations across the tropical Pacific Ocean. Previously, *Busalacchi et al.* [1994] compared the large-scale spatial structure of sea level observed by TOPEX/POSEIDON during the first 17 months of the mission with gridded fields of dynamic height from the entire TOGA-TAO array for 8°N-8°S and 95°W-137°E. Although an examination of the basin-scale variability was possible in that study, a quantitative pointwise intercomparison was precluded by the distribution of the TOPEX/POSEIDON ground tracks relative to the TAO mooring locations as well as the time-space decorrelation scales used in the optimal interpolation technique. Here we focus more on the time domain and thereby complement this previous examination of the spatial structure (more recently expanded upon by *Menkes et al.* [this issue]). A related paper by *Katz et al.* [this issue] describes the processing and analysis of the inverted echo sounder subset of observations taken as part of this experiment and the validity and limitations

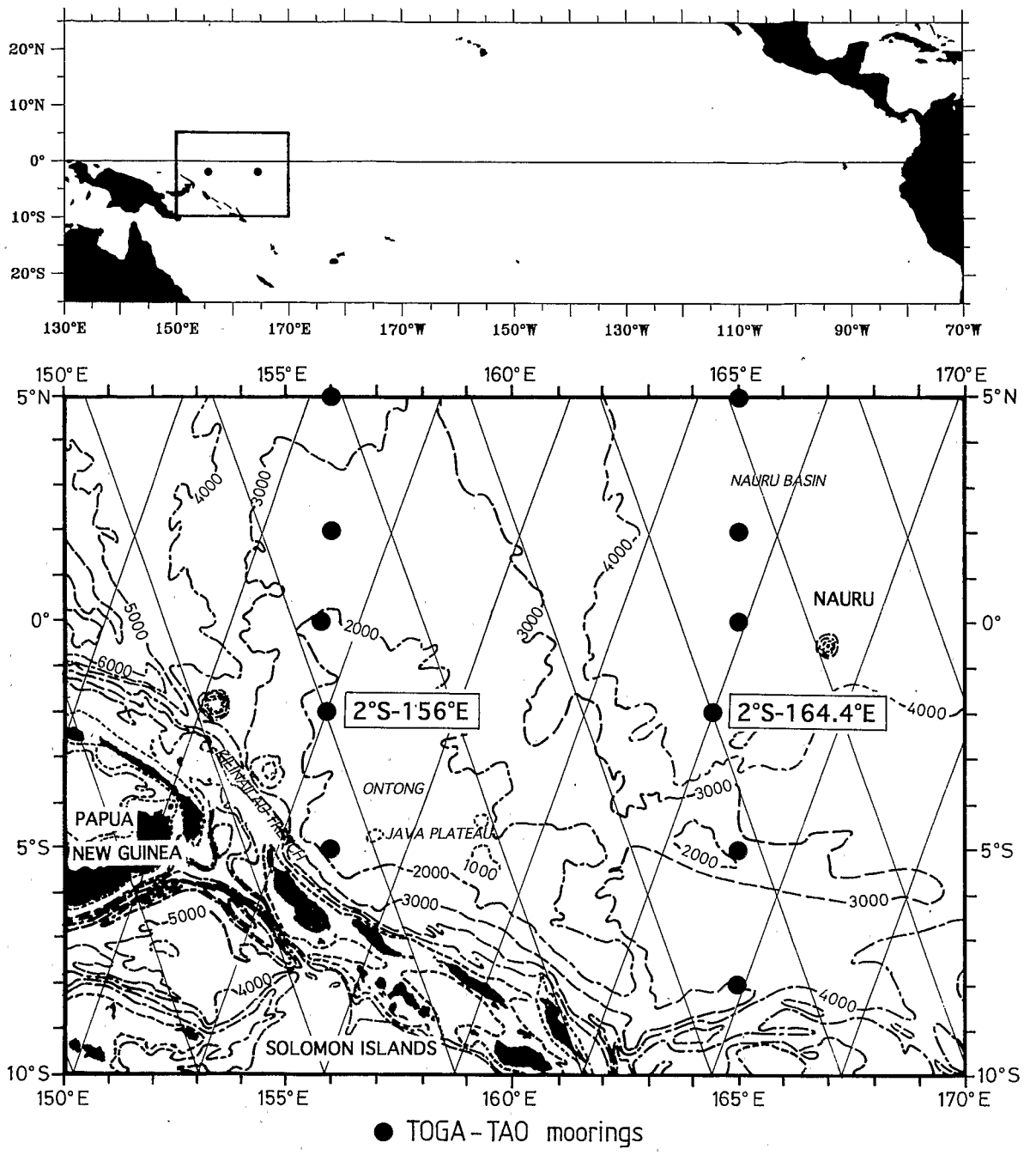

Figure 1. Locations of the two TOGA-TAO validation moorings at 2°S-156°E and 2°S-164.4°E. Superimposed are TOPEX/POSEIDON tracks and bathymetry contours in meters.

of this particular measurement technique when used to estimate changes in sea surface height.

The purpose of this paper is to present what may be one of the most precise estimates of sea level variability ever obtained in the open ocean. These in situ measurements of sea level are compared against instantaneous and low-pass-filtered observations from TOPEX/POSEIDON and placed in the context of the larger regional-scale variability. Discrepancies between the in situ and satellite measurements are described in terms of the physical processes at work in the area, the spectral content of the oceanic signal that TOPEX/POSEIDON is subsampling, and the environmental corrections needed to process the altimeter data. In section 2 the experimental design and the manner in which the data were processed are presented. The nature of the in situ variability observed at the two mooring sites is described in section 3 in terms of the regional context, the high-frequency variability, and low-frequency fluctuations. Section 4 follows with the intercomparison of the TOPEX/POSEIDON sea level variability with that observed in situ. Discussion and conclusions are presented in section 5.

2. The Experiment, Data Processing

This section summarizes the experimental design, instrumental configuration, operations at sea, and data processing for our validation experiment. More detailed information can

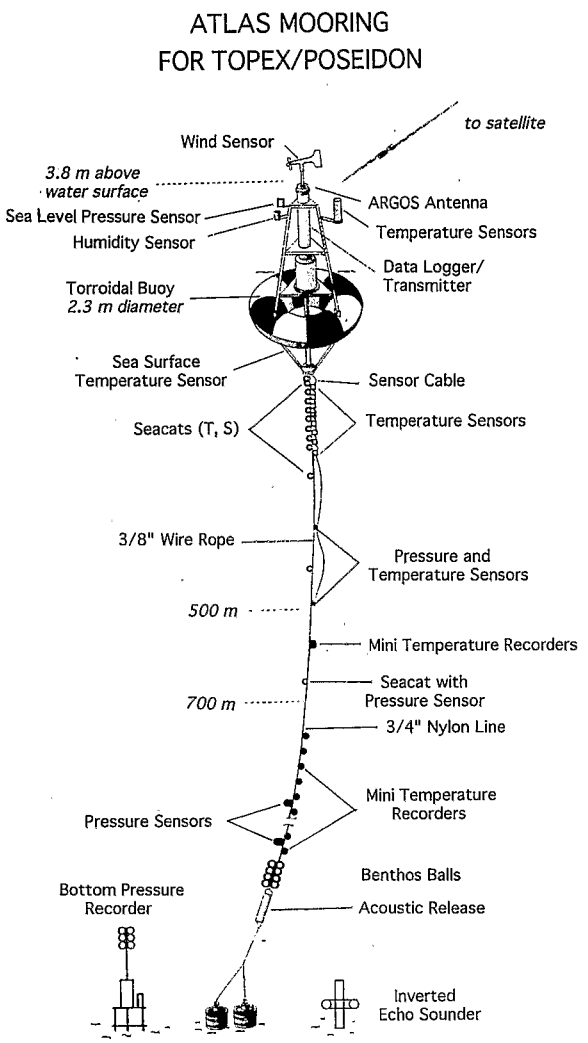

Figure 2. ATLAS mooring design, with additional instruments along the line (Seacats, mini temperature recorders, Benthos glass balls) and on the bottom (inverted echo sounder and bottom pressure recorder).

be found in a corresponding technical report [*Gourdeau et al.*, 1995].

2.1. Experimental Design

The ATLAS moorings [*Hayes et al.*, 1991] are currently equipped with wind, air temperature, relative humidity and sea surface temperature (SST) sensors, a thermistor chain composed of 10 temperature sensors (25–500 m), and two pressure sensors (300 and 500 m). The number and vertical distribution of additional temperature and salinity sensors along the mooring lines were determined through a sampling study based on 13 and 57 deep CTD casts made from 1984 to 1990, respectively, at and near 2°S-165°E. Surface dynamic heights relative to the bottom were calculated from a series of discrete T-S points subsampled from the CTD profiles at the sensors' depths and compared with their values using the complete CTD profiles. Different calculations, made with various array designs, resulted in an estimated standard error of less than 1 dynamic centimeter (dyn. cm) for the array used at sea. Because of important salinity variations in the first 500 m [*Delcroix et al.*, 1987], 10 thermosalinograph Seacat units were needed midway between pairs of standard ATLAS temperature sensors. Salinity at the ATLAS temperature sensors was computed by vertically interpolating the Seacat time series. From 500 m to the bottom (1739 m at 2°S-156°E, 4400 m at 2°S-164.4°E), water mass variations are small enough to use one Seacat at 750 m and several mini temperature recorders (MTRs). Salinity at the MTR depths was obtained by using a mean T-S relationship.

Table 1. Error Budget at 2°S-156°E

Error Type	rms Difference, dyn. cm
Vertical sampling	0.9
Derived salinity	0.4
Instrumental	0.4
Vertical displacement	0.3
Σ baroclinic	1.1

2.2. Instruments

Two ATLAS moorings at 2°S-156°E (1739 m depth, on the Ontong Java Plateau) and 2°S-164.4°E (4400 m depth, in the abyssal plain) were deployed from September 11, 1992, to February 22, 1993, and from August 26, 1992, to March 22, 1993, respectively. In addition to the standard ATLAS sensors, the following instruments were installed (Figure 2): (1) on the surface buoy, one Aanderaa surface pressure recorder at 2°S-156°E and 2°S-164.4°E; (2) along the lines, 16 thermosalinograph Seacats, (SB-16) at 2°S-156°E (two with pressure sensors), 11 Seacats at 2°S-164.4°E (two with pressure sensors),

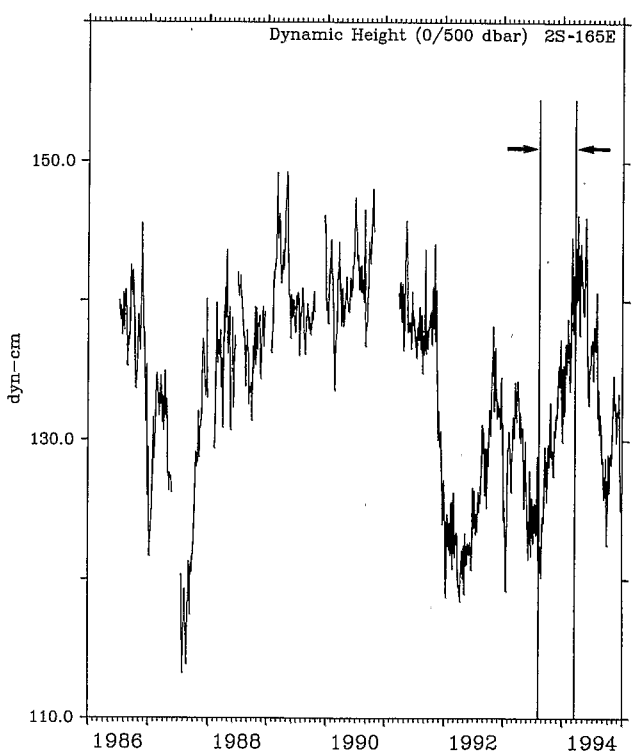

Figure 3. The 5-day mean sea surface dynamic height time series (1986–1994) relative to 500 dbar at 2°S-165°E calculated from the ATLAS thermistor chain and a mean T-S relation. The August 1992 to March 1993 period of the experiment is outlined within the two arrows.

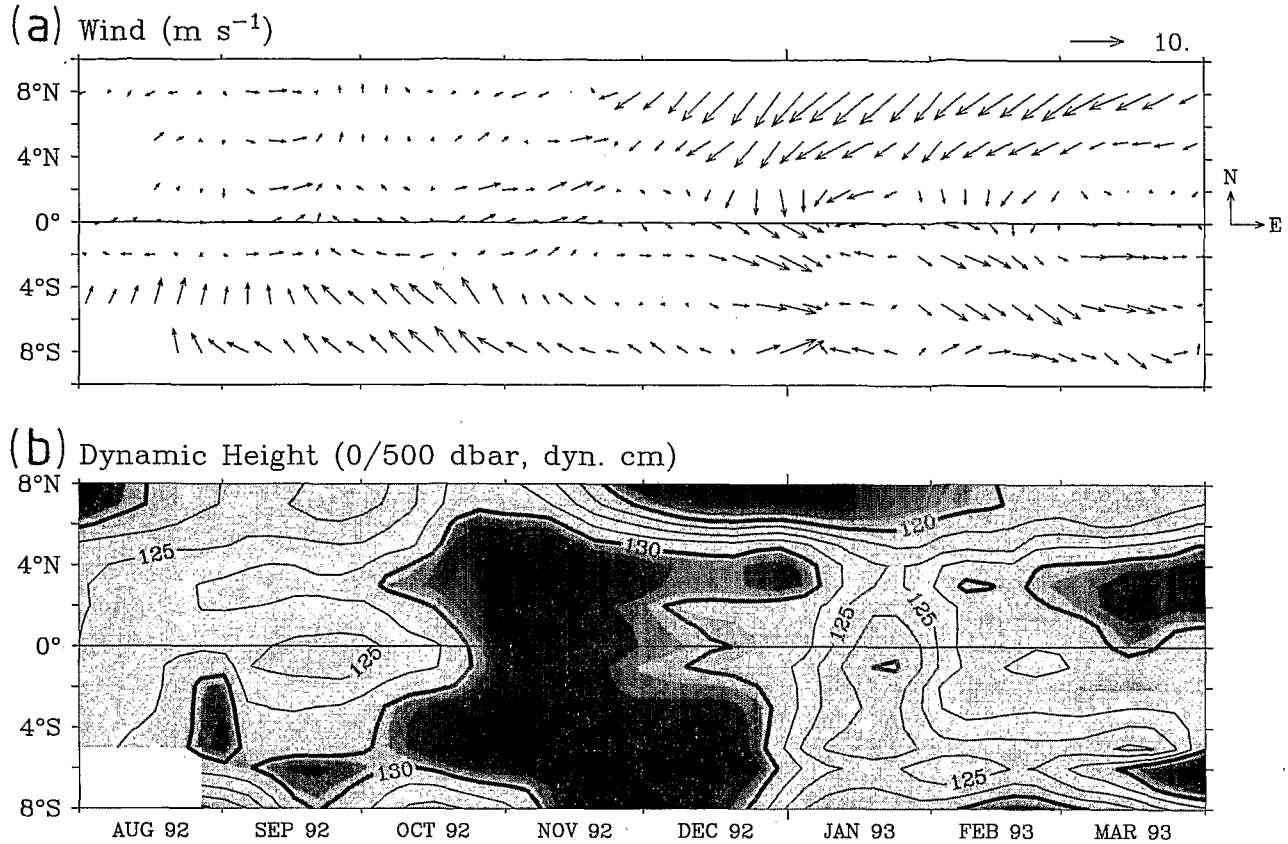

Figure 4. (a) The 5-day mean surface wind and (b) surface dynamic height (0/500 dbar) around 160°E during the period of the experiment. The data came from the TOGA-TAO moorings within 8°N-8°S and averaged across 156°E and 165°E. Dynamic height is calculated from the thermistor chain and a mean T-S relation; contours are every 2.5 dyn. cm.

five MTRs at 2°S-156°E, 12 MTRs at 2°S-164.4°E, one Aanderaa recorder (pressure and temperature) at 2°S-156°E, and two Aanderaa recorders at 2°S-164.4°E; and (3) on the bottom, one bottom pressure recorder (BPR) at 2°S-156°E, one BPR at 2°S-164.4°E, two inverted echo sounders (IESs) at 2°S-156°E, and one IES at 2°S-164.4°E. The greater number of Seacats on the ATLAS at 2°S-156°E was due to the addition of eight instruments provided by R. Lukas (University of Hawaii) as part of a COARE proposal to study the upper ocean thermohaline structure in the western equatorial Pacific.

2.3. Data Processing

On the 2°S-156°E mooring, no data were returned by one Seacat (45 m), and two Seacat data records were interrupted after 2 months of measurements (5 and 30 m). On the 2°S-164.4°E line, one Seacat time series was interrupted after 2 months (137 m) and the temperature sensor of the Seacat at 400 m failed after 1 month. At 2°S-164.4°E the MTRs stopped 10 days prior to recovery, and no data were returned by two of the 17 MTRs. For those instruments with complete records, pre- and postdeployment calibration differences were characterized by mean and standard deviation values, respectively, of −0.0013 and 0.0016°C for Seacat temperature, 0.0063 and 0.0227 practical salinity units (psu) for Seacat salinity, and 0.0042 and 0.0057°C for MTR temperature. The small difference between the pre- and postcalibrations of each sensor was used to correct the time series through a simple linear interpolation in time.

Owing to an unprotected memory battery drain, all Aanderaa pressure and temperature data were lost. Continuous (7.5-min sampling) surface sea level pressure within 15 n. mi. (28 km) of the 2°S-156°E ATLAS mooring was made available from October 21, 1992, to March 4, 1993, by R. Weller (Woods Hole Oceanographic Institution) as part of a COARE proposal to study air-sea flux exchange from the Improved Meteorological Package (IMET) mooring.

Since our experiment was based on the determination of accurate surface dynamic heights from the two moorings, very careful subjective and objective data editing was undertaken. Most of the Seacat sensors had the same sample rate (5 min) as the MTRs. A few Seacat data sets (e.g., those with pressure sensors) had a sample rate of 10, 20, or 30 min. These were interpolated to a common 5-min sampling using a technique which took into account the high-frequency information from the surrounding Seacat sensors. The 10 ATLAS thermistor chain sensors provided daily mean temperature in real time; they were interpolated to the common 5-min sample rate through another similar technique which took into account the high-frequency information from the Seacat sensors surrounding each ATLAS temperature sensor. Interrupted data records from a few sensors were extrapolated and interpolated in time using a combination of the initial data and the information from surrounding sensors [*Gourdeau et al.*, 1995].

All of the sensors on the mooring lines were subject to vertical displacement, mainly due to horizontal motion of the

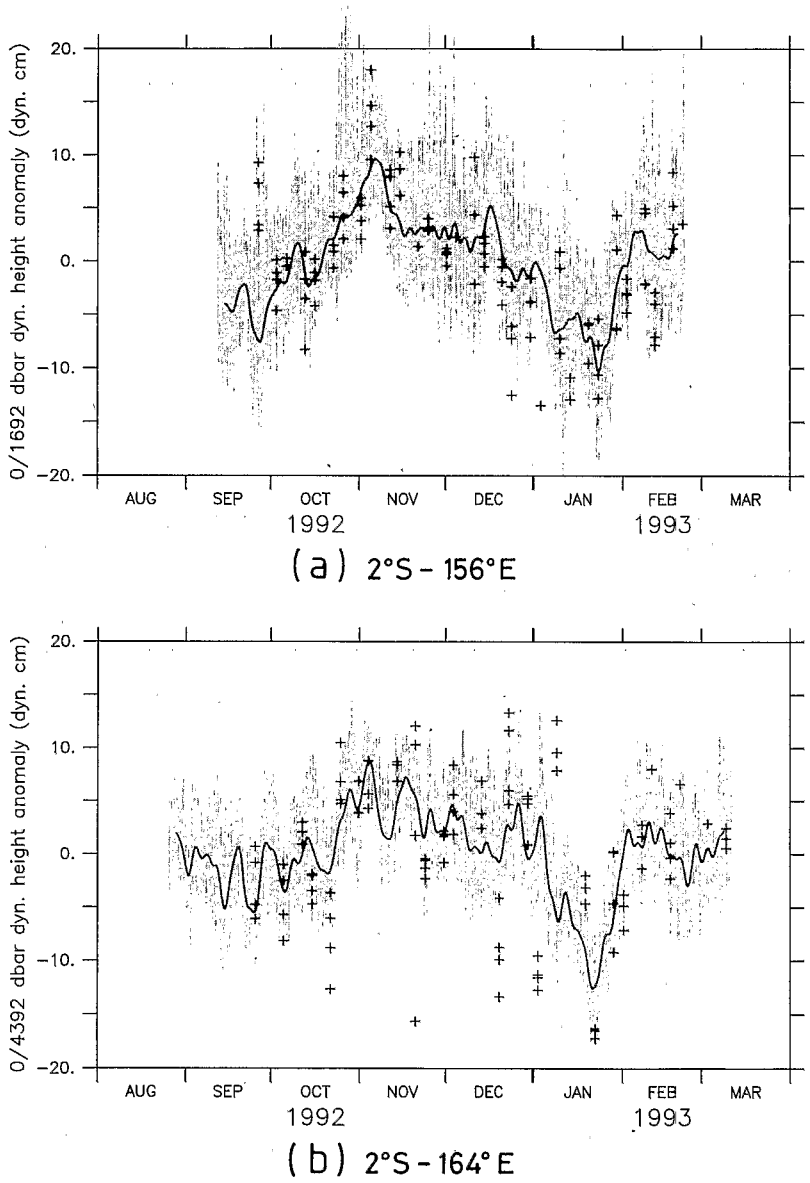

Figure 5. Original 5-min surface dynamic height (thin lines) and its low-pass-filtered (5-day Hanning filter, thick lines) time series at (a) 2°S-156°E and (b) 2°S-164.4°E. Superimposed are the 1-s sea level data of the eight points of TOPEX/POSEIDON measurement (pluses) nearest to the mooring sites. All time series are anomalies relative to the period of measurements.

buoy (e.g., low-frequency currents, tidal motion). At 400 m (750 m) the standard deviation of the vertical excursion was 2 m (4 m) with occasional extreme excursions of 6 m (15 m). Knowing that these vertical displacements may introduce additional error in the final dynamic height calculations, they have been taken into account at each time step and at each sensor location by estimating the shape of the mooring line using the pressure sensors at 300, 400, 500, and 750 m.

For the sensors without conductivity (standard ATLAS and MTR) the salinity in the first 750 m was deduced from the surrounding Seacats, and below 750 m a mean T-S relationship was used. The mean T-S at the two sites were constructed from the mean of 57 surface-to-bottom CTD casts taken from 1984 to 1990 around 2°S-164.4°E and from the mean of the 18 CTD casts taken from surface to bottom at 2°S-156°E during the repetitive 5°N-5°S COARE–Période d'Observations Intensives (POI) cruise [*Eldin et al.*, 1994]. The net result of processing these data sets was temperature, salinity, and depth time series every 5 min at 28 levels from September 12, 1992, to February 22, 1993 (163 days), for the 2°S-156°E mooring (1739 m depth) and at 32 levels from August 26, 1992, to March 11, 1993, (197 days) at 2°S-164.4°E (4400 m depth).

An estimate of the different errors entering into our final surface dynamic height calculations was determined. It was based mainly on a sensitivity study using the 18 CTD casts made at 2°S-156°E during the COARE-POI cruise. The CTD casts were collected between December 8, 1992, and February 23, 1993, a period which encompassed half of the time of our validation experiment. Additional error calculations were also done using the mooring data after their processing. The resulting 1.1 dyn. cm total error at 2°S-156°E (Table 1) is probably underestimated if applied at 2°S-164.4°E, given the coarse res-

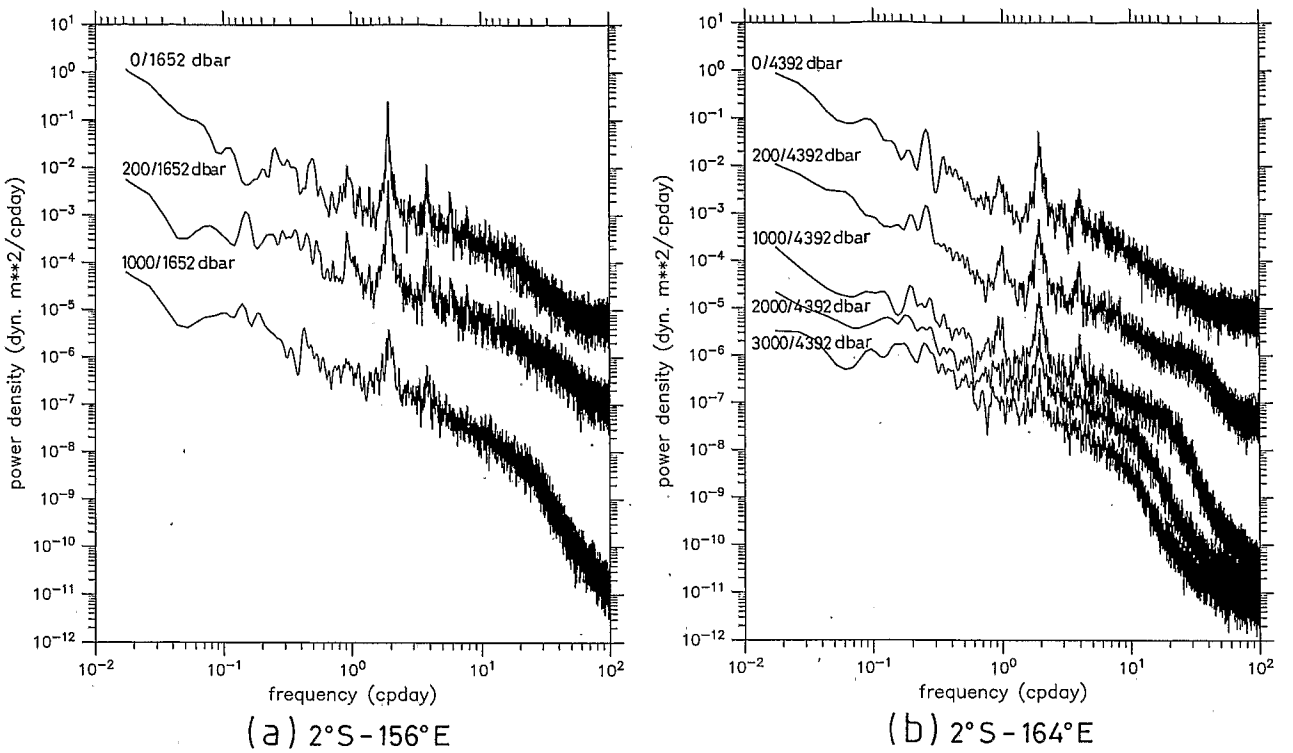

Figure 6. Spectra of dynamic height time series relative to the bottom at different levels at (a) 2°S-156°E and at levels 0, 200, and 1000 dbar and (b) 2°S-164.4°E and at levels 0, 200, 1000, 2000, and 3000 dbar. The spectra are shifted for clarity.

olution of the sensors over a larger depth (4400 compared with 1739 m) and the imprecise determination of vertical displacements of the sensors below the last 750-m pressure sensor [*Gourdeau et al.*, 1995]. However, given the small dynamic height signal at great depth (see section 3) and in view of the numbers in Table 1, the error in surface dynamic height at 2°S-164.4°E is likely to be of the order of 1.5 dyn. cm.

The BPR systems acquire average pressure each 15 s and have been used to measure tsunamis, tides, and seasonal phenomena to an accuracy of 1-mm equivalent seawater head at instrumental depths of 6000 m [*Eble and Gonzalez*, 1991; *Boss and Gonzalez*, 1994]. Calibration is highly stable; BPR-derived tidal constituents at one station were shown to be constant for more than 5 years [*Mofjeld et al.*, 1995]. The pressure time series was edited, converted to equivalent water levels by using vertically averaged local density and gravity values, subjected to a Lanczos-square 2-hour low-pass filter, subsampled to provide hourly values, and harmonically analyzed for 59 tidal constituents [*Foreman*, 1977]. Because accurate tide estimates are key to this experiment, we performed direct tests of potential errors introduced by filtering, hourly subsampling, and instrumental drift apparent in the initial portion of the time series. A test series was generated of unit amplitude, 15-s sampling, and 3.1-hour period (the shortest period constituent in our tidal analysis, M_8). Filtering left the amplitude and phase unchanged; hourly subsampling and harmonic analysis produced a constituent amplitude reduced by 12%. Since all constituents with periods less than 8 hours possessed amplitudes smaller than 3 mm, the effect of the filtering and subsampling was negligible. We then modeled and removed an exponential drift function fit to the data [*Watts and Kontoyiannis*, 1990], and a second tidal analysis produced tidal constituents essentially identical to the originals. However, the difficulty in removing the instrumental drift compromised the determination of the low-frequency geophysical signal.

2.4. TOPEX/POSEIDON Data

The TOPEX and POSEIDON altimeter data and their environmental corrections used in this study come from an enhanced geophysical data record (GDR) produced by the NASA Goddard Space Flight Center (GSFC) ocean altimetry group (C. Koblinsky, personal communication, 1994). In this data set the GDRs for the TOPEX and POSEIDON altimeters have been interpolated every 6 km to fixed points along track and referenced to the location of the cycle 17 ground track. Since no altimetric measurement was made exactly over a mooring site, a maximum of eight TOPEX/POSEIDON retrievals nearest to the two mooring sites were used (i.e., four along descending and four along ascending tracks and within 18 km from the moorings) in the instantaneous comparisons between the 1-s TOPEX/POSEIDON sea level and the 5-min surface dynamic heights. The POSEIDON data have been merged with the TOPEX data by removing a 13.6-cm bias [*Nerem et al.*, 1994] which can vary by several centimeters [*Ménard et al.*, 1994]. The first 19 10-day cycles are considered here, covering the period from September 25, 1992, to March 30, 1993. For the purposes of evaluating the satellite versus the in situ sea level time series, the barotropic tides were removed from the altimeter data using the tidal corrections from several tide models that were at our disposal, i.e., enhanced modified *Schwiderski* [1980], *Cartwright and Ray* [1990], and *Ray et al.* [1994]. The inverse barometer effect due to atmospheric pressure loading was accounted for using the GDR correction based on the European Centre for Medium-Range Weather

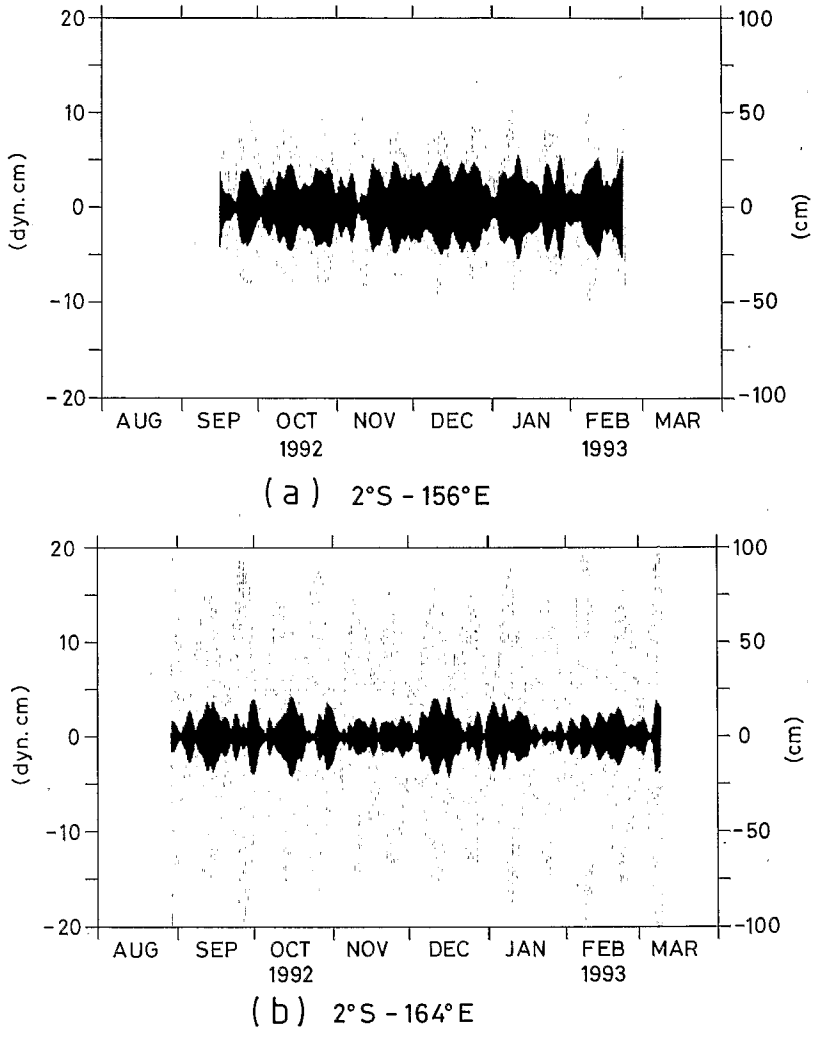

Figure 7. Complex demodulation (around 12.5 hours) of the sea surface relative to bottom dynamic height (thick lines evidenced as dark shading) and of the barotropic tides (thin lines evidenced as light shading) at (a) 2°S-156°E using 13 constituents of the *Schwiderski* [1980] tide model and (b) 2°S-164.4°E using the 59 constituents of the tides observed with the bottom pressure recorder. For convenience, the baroclinic and barotropic tides are represented with a 1 to 5 ratio, i.e., within ±20 dyn. cm (left axes) and within ±100 cm (right axes).

Forecasts (ECMWF) atmospheric surface pressure analysis and on sea level pressure observed during TOGA-COARE near the 2°S-156°E mooring.

3. Description of Major Observed Phenomena

3.1. Regional Low-Frequency Context

The field phase of this study (August–September 1992 to February–March 1993) took place between the two major warming episodes in the eastern equatorial Pacific which characterized the 1991–1993 El Niño [*McPhaden*, 1993]. Figure 3, which represents the longest sea surface dynamic height measurement in the western Pacific, places our study into a more general context. In the western equatorial Pacific, the 1986–1987 and 1991–1994 El Niño were characterized by a drop of sea level of more than 20 dyn. cm. The 1988–1989 La Niña was also notable, with a sea level rise which picked up in early 1989 by about 10 dyn. cm. During boreal fall/winter and especially during the onset of El Niño, winds in the western Pacific were punctuated by frequent westerly wind bursts often associated with enhanced 40- to 60-day intraseasonal *Madden and Julian* [1971] wave activity [*Kessler et al.*, 1995]. These westerly wind bursts excited a series of eastward propagating, low baroclinic mode equatorial oceanic Kelvin waves which were detected in both the TOGA-TAO time series [*Kessler et al.*, 1995] and in the Geosat and TOPEX/POSEIDON altimeter data [*Delcroix et al.*, 1994; *Busalacchi et al.*, 1994]. Recent work supports the idea that these waves may be important in the dynamics of El Niño [*Kessler and McPhaden*, 1995; *Picaut and Delcroix*, 1995].

To place our study in the context of regional-scale variability occurring in the western equatorial Pacific during August 1992 to March 1993, Figure 4 shows the surface wind and dynamic height time series between 8°N and 8°S in the longitude range 156°E-165°E. Southeast trade winds prevailed in the latter part of 1992 south of the equator, giving way to a monsoonal circulation in early 1993 with northeasterlies north of the equator and northwesterlies south of the equator (Figure 4a). Superimposed on this seasonal circulation were four episodes of intensified westerly winds within a few degrees of the equator.

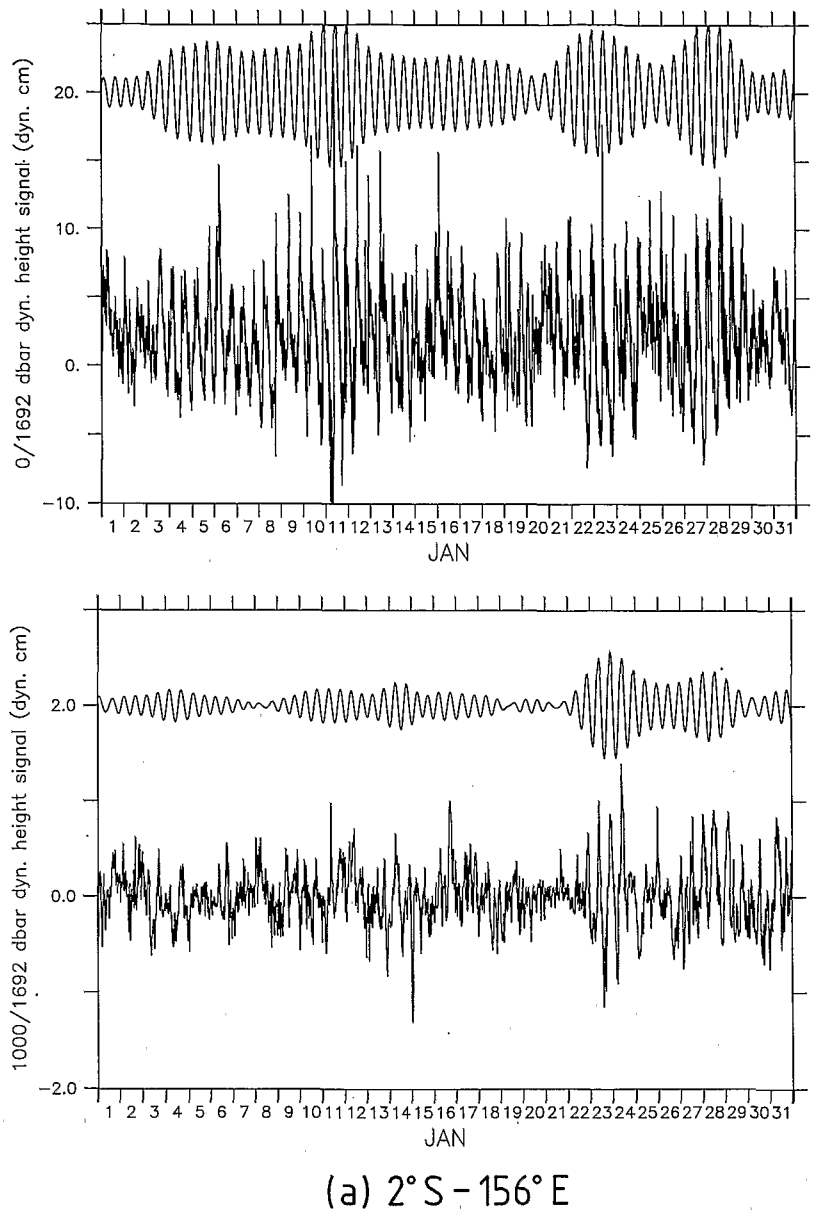

Figure 8. High-pass filtered (5-day Hanning filter) and complex demodulation (around 12.5 hours) time series of the dynamic height data relative to the bottom in January 1993 at (a) 2°S-156°E at the (top) surface and (bottom) 1000 dbar and (b) 2°S-164.4°E at the (top) surface and (bottom) 3000 dbar.

These episodes, each of which lasted 2–4 weeks, took place in September, October–November, December–January, and February–March. The strongest of these westerly episodes occurred in December–January, with 5-day mean wind speeds up to 5 m s^{-1}. The September–November events tended to be stronger north of the equator, whereas the December–March events were stronger south of the equator, reflecting in part the structure of the mean seasonal cycle on which they were superimposed.

The regional sea level response to these westerly wind episodes varied from one episode to the next between 156°E and 165°E, most likely because of the different spatial structures (both latitudinal and longitudinal) of the wind forcing in relation to the mooring sites. Dynamic height, for example, rose 10 dyn. cm within a few degrees of the equator in association with the October–November westerly wind burst (Figure 4b). This was followed in December–January by a rapid decrease of 10 dyn. cm associated with a rise of the thermocline in response to the sudden wind changes from westerly to easterly [*Eldin et al.*, 1994]. The September and February–March westerly wind episodes, on the other hand, had a much less pronounced impact on the surface dynamic height.

In addition to these intraseasonal dynamic height variations, there was also a large, 15 dyn. cm decrease in sea level near 8°N from November to January, which may have been associated with seasonal cooling during the boreal fall-winter. Seasonal dynamic height variations were not so evident in the southern hemisphere, perhaps because the seasonal cycle there was obscured by intraseasonal and/or interannual variations, the latter of which lead to a sea level lower than normal by 10–15 cm in the western Pacific throughout the period of our study.

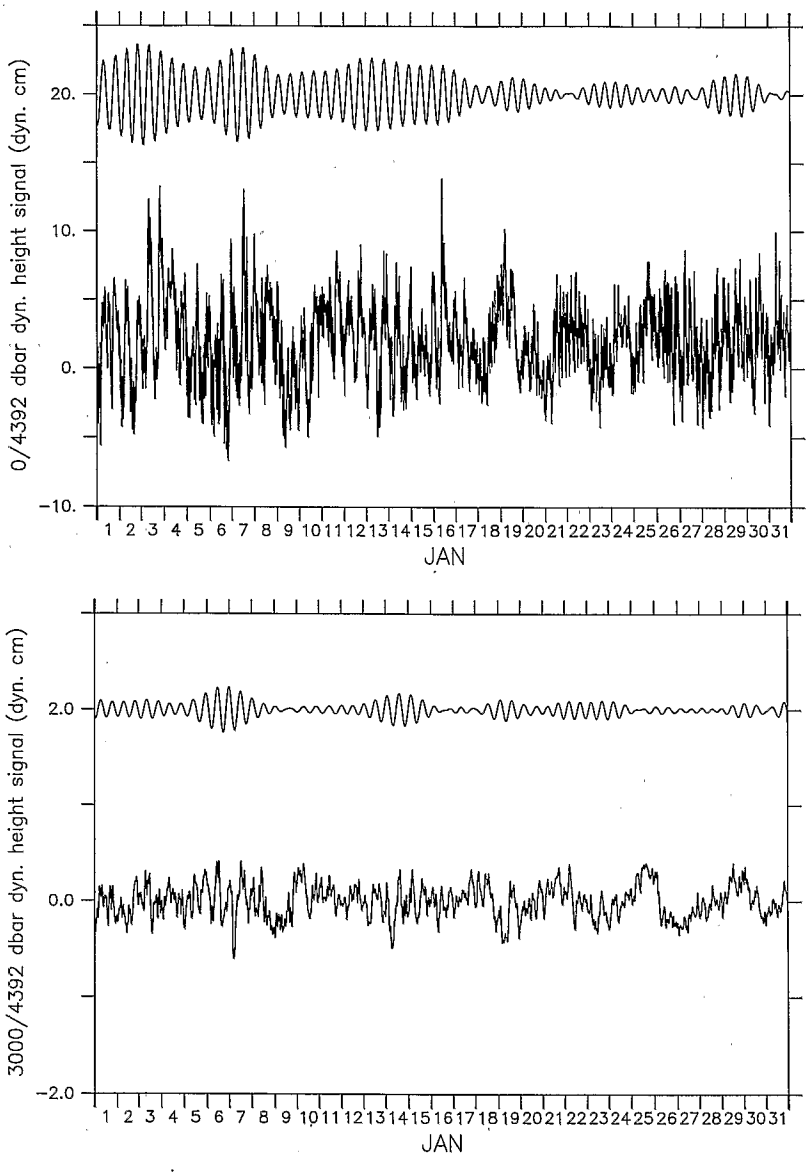

Figure 8. (continued)

3.2. Spectrum of Variability at the Validation Sites

Time series of dynamic height at the surface relative to the bottom calculated at 5-min intervals are presented in Figure 5. As can be seen, the dynamic height at both locations is a combination of high-frequency and low-frequency variations. The high-frequency variability in surface dynamic height is distinctly greater at 2°S-156°E than at 2°S-164.4°E. It is also worth noting that the range of variation at this location encompasses most of the eight 1-s TOPEX/POSEIDON sea level measurements nearest to the mooring sites. The implication for these high-frequency fluctuations relative to the 10-day TOPEX/POSEIDON sampling is discussed in sections 4 and 5.

Spectral analysis of the dynamic height series at different levels (Figure 6) reveals, in the high-frequency band, the dominance of a strong semidiurnal signal with surrounding energy around 4, 6, and 24 hours. These signals are dominant in the surface layer and remain at depth. In the lower-frequency band there is some energy around 4 days, 10 days, and longer periods. This spectral analysis suggests a separation between high- and low-frequency variability at around 2 days. Figure 5 illustrates the separation between low- and high-frequency variability in the surface dynamic height from the two moorings. Low-frequency variability is similar, with a standard deviation of 4.3 dyn. cm at 2°S-156°E and 3.9 dyn. cm at 2°S-164.4°E. As noted above, high-frequency surface variability (period less than 2 days) is definitely of larger magnitude at the 2°S-156°E site, with a standard deviation of 3.5 dyn. cm compared with 2.7 dyn. cm at 2°S-164.4°E.

3.3. High-Frequency Variability at the Validation Sites

Most of the high-frequency variability seen in surface dynamic height is associated with internal tides with the M_2 and S_2 constituents being dominant. Complex demodulation analysis around 12.5 hours indicates these dynamic height variations associated with the semidiurnal internal tides are most energetic in the surface layer and confirms their presence all

the way to the bottom (Figures 6, 7, and 8). They have larger amplitude at the shallow site (1739 m at 2°S-156°E) than on the abyssal plain (4400 m at 2°S-164.4°E), with standard deviations of 2.3 and 1.4 dyn. cm, respectively. Over the 6–7 months of our experiment they appear as a superposition of wave trains of 5- to 15-day duration. Some similarities between the complex demodulation of the surface dynamic height and barotropic tides at the two sites suggest a possible relation between internal tides and spring tides in setting up these wave trains (Figure 7). This relation between baroclinic and barotropic tides is more obvious at the shallower 2°S-156°E site, where the internal tides are stronger and, apparently, the barotropic tides are smaller (with only 21 days of BPR measurements at 2°S-156°E the modeled *Schwiderski* [1980] tides are used as a proxy for the observed tides). The temporal and spatial variability of these wave trains is examined in detail over a specific month (e.g., January 1993) through the representation of the original high-frequency variability and its complex demodulation (Figure 8). Vertical coherence varies with time, but both amplitude and duration are found to generally decrease with depth.

A detailed examination of the time series reveals that on some days, high-energy solitary waves, related to the semidiurnal internal tides, are clearly detectable at the shallower 2°S-156°E site (Figure 9). No such evidence is found on the abyssal plain at 2°S-164.4°E during the 6-month duration of the experiment. The strongest solitary waves exhibit variations that are coherent and in phase from surface to bottom. Within less than an hour they can give rise to isopycnal displacements of up to 100 m below the pycnocline and to sea surface displacements of up to 30 dyn. cm. Ship radar observations near the 2°S-156°E site during the COARE intensive observation period showed that they were probably coherent over 20–30 km along crest (R. Pinkel, personal communication, 1994). All these observations strongly suggest that the proximity of rough bottom topography may be a dominant factor in the generation of both the stronger internal tides and solitons at 2°S-156°E.

3.4. Low-Frequency Variability at the Validation Sites

With the large space scale of low-frequency equatorial phenomena [e.g., *Meyers et al.*, 1991] the two validation sites exhibit very similar low-frequency surface to bottom dynamic height variability, especially on monthly timescales observable by the 10-day repeat altimetric measurements (Figure 10). As noted in section 3.1, surface dynamic height is dominated by the successive sea level rise associated with the October–November westerly wind burst and the sea level fall associated with the January wind change from westerly to easterly. Most of this signal is dominated by variations in the upper 500 m. Specifically, the dynamic height standard deviation for 500-dbar relative to bottom is 0.6 and 0.7 dyn. cm compared with 4.1 and 3.4 dyn. cm for surface relative to bottom, respectively, at 2°S-156°E and 2°S-164.4°E (Figure 10).

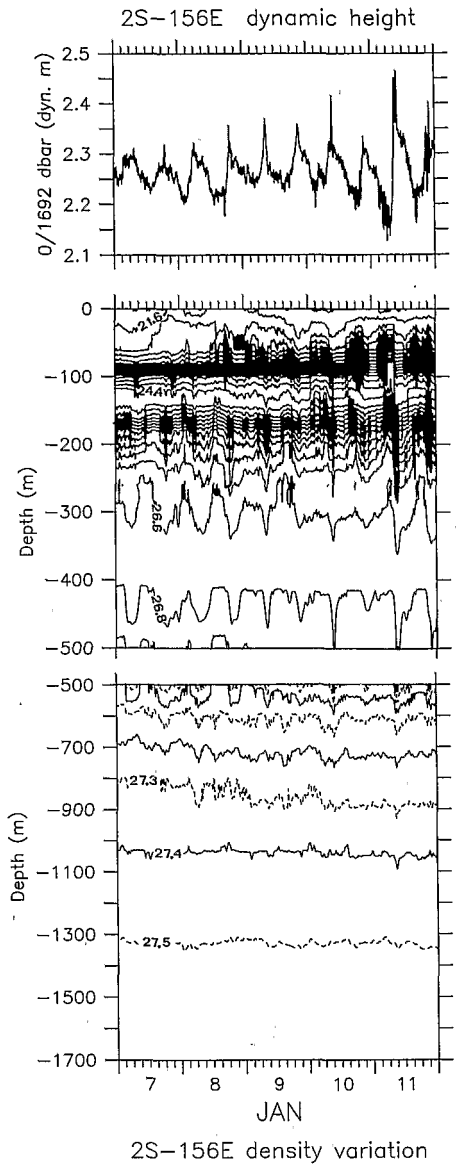

Figure 9. Examples of strong solitons associated with the semidiurnal tides at 2°S-156°E on January 7–11, 1993. (top) Sea surface dynamic height relative to bottom. (middle) Vertical density structure within 0–500 m, and (bottom) vertical density structure within 500 m and the bottom.

4. Intercomparison Study

4.1. Instantaneous Comparison

Given the general overlap of the 1-s TOPEX/POSEIDON sea level retrievals and the 5-min surface dynamic height evidenced in Figure 5 (especially at 2°S-156°E), it is of interest to determine the level of error in the instantaneous comparison between the satellite and in situ sea level measurements. Even if the TOPEX/POSEIDON mission was designed mostly for large-scale studies, this exercise may be informative in terms of instantaneous corrections applied to the altimetric measurements (e.g., tidal and inverse barometer corrections).

The 1-s TOPEX/POSEIDON sea level anomalies at a given pass of the satellite over a mooring site are compared with the corresponding in situ 5-min surface dynamic height anomalies. With the satellite flying over a site twice every 10-day cycle, a total of 27 passes were available during our experiment, of which three (six) passes were made by the POSEIDON altimeter at 2°S-156°E (2°S-164.4°E). We considered at first the eight points of measurement closest to a site (i.e., within 18 km from a site). For a specific point the TOPEX/POSEIDON anomaly is defined relative to the mean of all 1-s measurements at this point available over the duration of the experiment (i.e., mean calculated over 14 descending or 13 ascending tracks). In the same way, the dynamic height anomaly is defined relative to the mean of the 5-min dynamic heights cor-

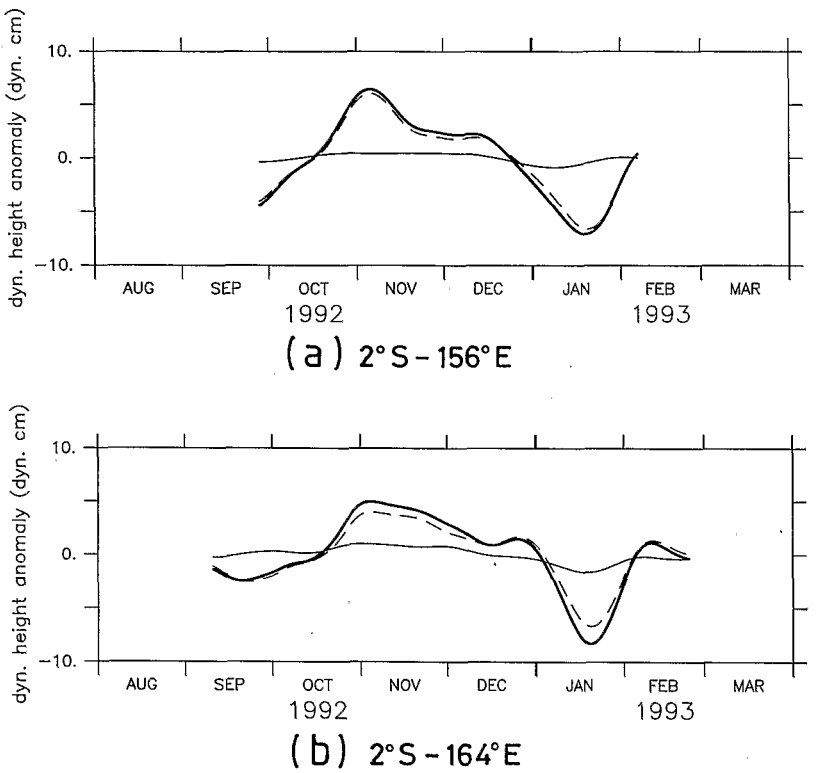

Figure 10. Low-frequency (30-day Hanning filter) dynamic height time series of surface to bottom (thick solid line), surface/500 dbar (dashed line), and 500 dbar/bottom (thin solid line) at (a) 2°S-156°E and (b) 2°S-164.4°E.

responding to the previous TOPEX/POSEIDON measurements. Since tides were measured from the BPR at 2°S-164.4°E and atmospheric sea level pressure measured close to 2°S-156°E, the tidal and atmospheric sea level pressure corrections applied to the TOPEX/POSEIDON data set are considered separately.

With the enhanced GDR provided by the NASA GSFC ocean altimetry group, three tidal corrections were included. They come from the enhanced modified *Schwiderski* [1980], *Cartwright and Ray* [1990], and *Ray et al.* [1994] models. From these three models, 13, 5, and 4 tidal constituents, respectively, were available at 2°S-156°E and 2°S-164.4°E (courtesy of C. Le Provost). With 6 months of BPR measurements at 2°S-164.4°E, 59 tidal constituents were calculated ranging from M_8 to M_{sm}. The first 13 constituents are listed in Table 2, and the comparisons between the BPR and the various tide models are summarized in Table 3. All three tide models used the long-period equilibrium tides. These long periods contribute weakly to the total tidal signal, with 1.5 cm standard deviation as compared with 46 cm standard deviation for the hourly BPR record. However, as discussed by *Wunsch* [1967] and *Miller et al.* [1993] in the tropical Pacific, these semimonthly and monthly long-

Table 2. Period, Amplitude, and Phase of the Major Tidal Constituents at 2°S-164.4°E

		Bottom Pressure Recorder		Schwiderski Model		Cartwright and Ray Model		Ray et al. Model	
Constituent	Period, hours	Amplitude, cm	Phase, deg	Amplitude, cm	Phase, deg	Amplitude, cm	Phase, deg	Amplitude, cm	Phase, deg
M_2	12.42	52.2	146	47.8	144	52.2	141	54.1	141
S_2	12.00	28.5	160	27.4	159	27.0	150	30.9	153
K_1	24.00	15.4	62	15.0	61	15.2	54	15.3	58
N_2	12.66	10.8	146	9.0	145	10.7	144	...	...
O_1	25.82	9.2	41	8.6	40	9.2	35	8.5	42
K_2	11.97	8.5	154	7.3	155	...	...	...	...
P_1	24.07	4.8	60	4.9	61	...	...	...	...
L_2	12.19	2.1	138	1.4	148	...	...	...	...
μ_2	12.87	2.0	136	1.5	151	...	...	...	...
T_2	12.02	1.9	157	1.5	153	...	...	...	...
ν_2	12.22	1.9	146	1.7	145	...	...	...	...
Q_1	26.87	1.6	22	1.6	20	...	...	...	...
$2N_2$	12.63	1.6	136	1.3	152	...	...	...	...

Models are from *Schwiderski* [1980], *Cartwright and Ray* [1990], and *Ray et al.* [1994].

period tides are not exactly in equilibrium, with a 0.6 cm rms difference from the equilibrium tides. Therefore a BPR55 comparison (i.e., with M_{sm}, M_m, M_{sf}, and M_f omitted) was added in Table 3 as an additional reference for the comparisons between the tide models and the BPR. The 7.6 cm rms difference between BPR13 and BPR05 compared with the 2.0 cm rms difference between BPR13 and BR59 indicates that 13 constituents is a significant improvement in reproducing the tides at 2°S-164.4°E. Using only four or five of the major constituents (common to the three tidal models), we note that the Schwiderski model fits best the BPR (Table 3). This is probably due to its ability to reproduce better the observed S_2 constituent, as all three models result in an identical rms difference with the BPR when the S_2 constituent is moreover omitted from the comparisons. The radiational component of the S_2 constituent, measured with the BPR, is partly included in the Schwiderski model, as this model is the only one forced by tide gauge measurements. Keeping in mind that the Schwiderski model is the best to fit our BPR measurements with four constituents, we note that in its enhanced modified 13-constituent version the rms difference with BPR13 is 4.1 cm.

Spectral analysis of the sea level atmospheric pressure observed near the 2°S-156°E site clearly shows a strong semidiurnal signal, a diurnal signal, and some energy in the 4- to 7-day and 30- to 60-day band (the last corresponding to the *Madden and Julian* [1971] oscillation). The semidiurnal and diurnal signals correspond to the atmospheric tides of thermal origin [*Chapman and Lindzen*, 1970]. They are clearly evident within the tropics where atmospheric pressure is usually stable. Given the 6-hour window of data assimilation in the ECMWF model, they are probably poorly resolved in this model. In any case the inverted barometer correction applied to the altimetric measurements is not reliable for periods shorter than 2 days [*Ponte et al.*, 1991].

The instantaneous comparisons were done between the TOPEX/POSEIDON sea level anomalies and the sea surface dynamic height anomalies using the corrections issued from the three different tidal models (Table 4). Using the eight nearest points to the mooring sites, the rms differences are around 5–6 cm for all models. The rms differences decrease significantly if only the four nearest points of measurement are considered (i.e., two points of measurement along the descending and two points along the ascending tracks), especially using the *Schwiderski* [1980] tide model. Given the reduced number of POSEIDON measurements (3, 6 as compared to 24, 22 TOPEX measurements, respectively, at the 2°S-156°E and 2°S-164.4°E mooring sites), the adjustment (within a few centimeters) of the POSEIDON bias does not ameliorate the preceding results. However, the instantaneous comparisons improve a little if the POSEIDON information is removed, reducing the rms differences to 3.3 cm at 2°S-156°E and 3.7 cm at 2°S-164.4°E. The replacement of the tidal corrections included in the TOPEX/POSEIDON GDR by the observed tides (predicted from the constituents calculated from the BPR measurements at 2°S-164.4°E) does not improve all the previous results, even if all the 59 BPR constituents are used (M_{sm} to M_8). In that case we are assembling 1-s TOPEX/POSEIDON sea level with tidal corrections which cannot resolve periods shorter than 3.1 hours (M_8), and at this point we probably have reached the level of instantaneous error in tidal observations and models.

Table 3. The rms Difference Between the Predicted Tides Calculated With *N* Constituents Derived From the Bottom Pressure Recorder and the Three Tidal Models

BPR/BPR					BPR/S				BPR/CR			BPR/RSC	
N	55	13	5	4	*N*	13	5	4	*N*	5	4	*N*	4
59	1.5	2.0	7.9	11.1	59				59			59	
55		1.3	7.7	11.0	55				55			55	
13			7.6	11.0	13	4.1			13			13	
5				7.7	5		3.9		5	5.3		5	
4					4			3.6	4		5.3	4	4.7

Units are centimeters. S is Schwiderski model, CR is Cartwright and Ray model, and RSC is Ray et al. model.

Table 4. The rms Difference Between the 1-s TOPEX and POSEIDON Sea Level and the 5-min Dynamic Height Using the Eight and Four Sea Level Points Nearest to the Mooring Site and the Three Tidal Models

	2°S-156°E	2°S-164.4°E
8, all models	5–6	5–6
4, RSC	4.6	4.6
4, CR	4.2	4.1
4, S	3.6	4.4
4, S*	3.3	3.7

Units are centimeters. See Table 3 for model information.
*POSEIDON sea level data are not included.

Figure 11 depicts the comparison with the nearest four points of TOPEX and POSEIDON measurements. At 2°S-164.4°E the dispersion in POSEIDON measurements is evident, suggesting noisier measurements than with the TOPEX altimeter. The spectral characteristics of TOPEX and POSEIDON agree well at low wavenumbers, however, they differ at short wavelengths, POSEIDON spectra being more energetic. This is essentially due to the TOPEX tracker characteristics and to the way the acceleration correction is made on the GDR (P. Vincent, personal communication, 1995). Nevertheless, the dispersion of TOPEX measurements is also notable in December–January. During this period the winds were strong and varied in direction (Figure 4), and it is possible that the sea state correction, of significant amplitude (Figure 12), was not adequate. Note that Figure 12 is also characterized by a greater sea state correction with POSEIDON than with TOPEX [*Gaspar et al.*, 1994]. This correction is a function of the wind speed and of the significant wave height. Despite the 10-day sampling the altimetric winds seem to be in good accordance with the winds observed from the two ATLAS moorings (not shown), and it is probable that the correction associated with surface waves was not accurately determined from the altimeters in a sea exposed to varying winds.

The inverse barometer hypothesis was tested in two ways. Following the result of *Fu and Pihos* [1994] in the western tropical Pacific, a -0.4 cm mbar^{-1} correction factor instead of the traditional -1 cm mbar^{-1} factor was applied to the inverse ECMWF barometer correction included in the TOPEX/POSEIDON GDR. At 2°S-156°E the rms difference between the instantaneous comparison of the sea surface dynamic height and the altimeter sea level improves from 3.6 to 3.4 cm. Using the observed sea level atmospheric pressure near the 2°S-156°E mooring instead of the ECMWF pressure and the same -0.4 cm mbar^{-1} factor does not significantly change the

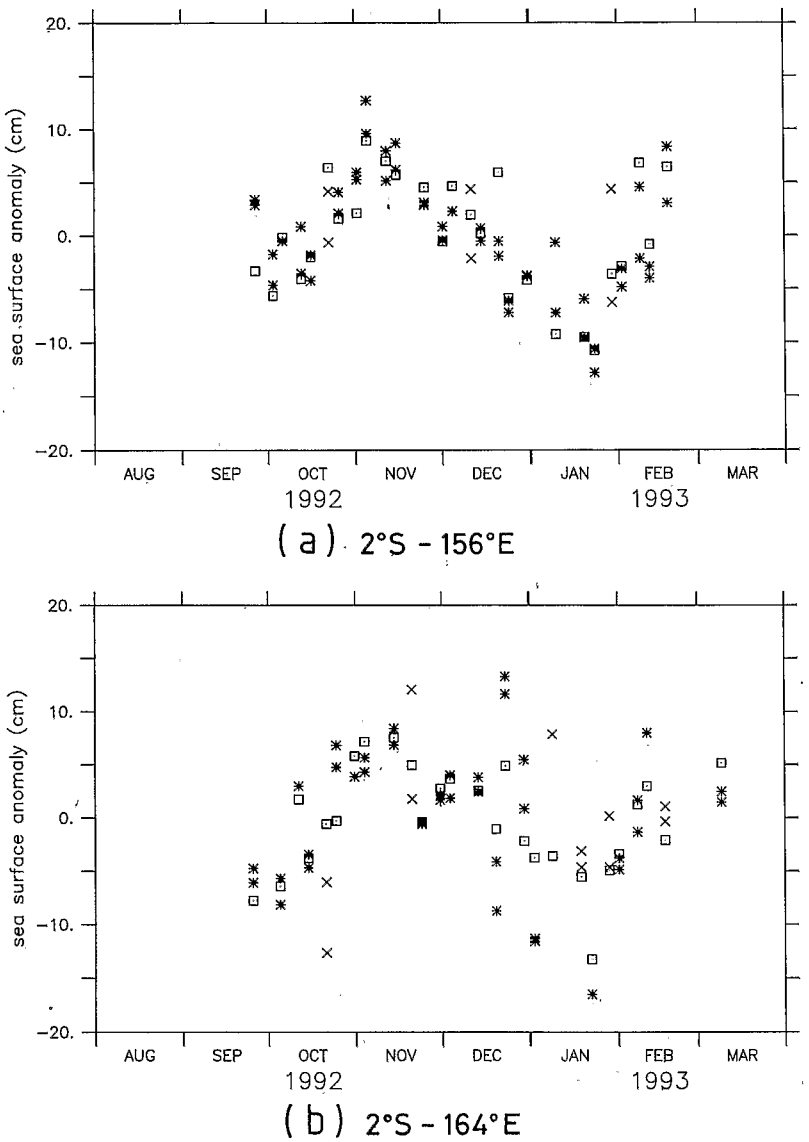

Figure 11. Instantaneous comparison between the 5-min sea surface dynamic height (squares) and the TOPEX (stars) and POSEIDON (crosses) sea level at the four nearest points to the mooring sites at (a) 2°S-156°E and (b) 2°S-164.4°E.

preceding result, with an rms difference of 3.3 cm. Essentially the same results were also obtained when we used the −1 cm $mbar^{-1}$ correction. This confirms the weakness of the correction associated with the sea level atmospheric pressure in the tropics.

In summary, our instantaneous comparison between TOPEX/POSEIDON sea level and sea surface dynamic height at the two mooring sites results in an rms difference of 3–4 cm. This is surprisingly good, knowing the numerous errors involved in such an instantaneous comparison. For example, we are comparing 5-min sea surface dynamic height with 1-s TOPEX/POSEIDON sea level, barotropic tidal models are in error by 3–5 cm rms [*Le Provost et al.*, 1995], the sea state correction is likely to be inadequate part of the time, and the inverse barometer correction should not be applied for periods shorter than 2 days [*Ponte et al.*, 1991].

4.2. Low-Frequency Comparison

Despite the encouraging results of section 4.1, with extreme sea surface dynamic height variation of up to 30 cm on time-scales as short as 1 hour, it is obvious that sampling error could be important, given the 10-day repeat coverage of TOPEX/POSEIDON. Hence we are interested in the extent to which the low-frequency dynamic height variability (Figure 10) can be accounted for with appropriate space-time averaging of the altimeter data.

To perform the low-frequency comparison, dynamic height data were averaged to produce daily means at both locations. Similarly, all TOPEX/POSEIDON data falling within an x degree longitude by y degree latitude box, centered on the mooring location, were averaged or interpolated into daily values, as the amount of spatial coverage varied according to the size of the box. A rectangle 20° longitude by 10° latitude was the minimum size resulting in nearly continuous daily series (94% of the days of the studied period have valid TOPEX/POSEIDON data). The percentage fell to 66%, 45%, and 35%, respectively, for the 15° × 3°, 10° × 3°, and 5° × 2° box, and the data were linearly interpolated to daily values. As an example, Figure 13 displays the daily time series of the

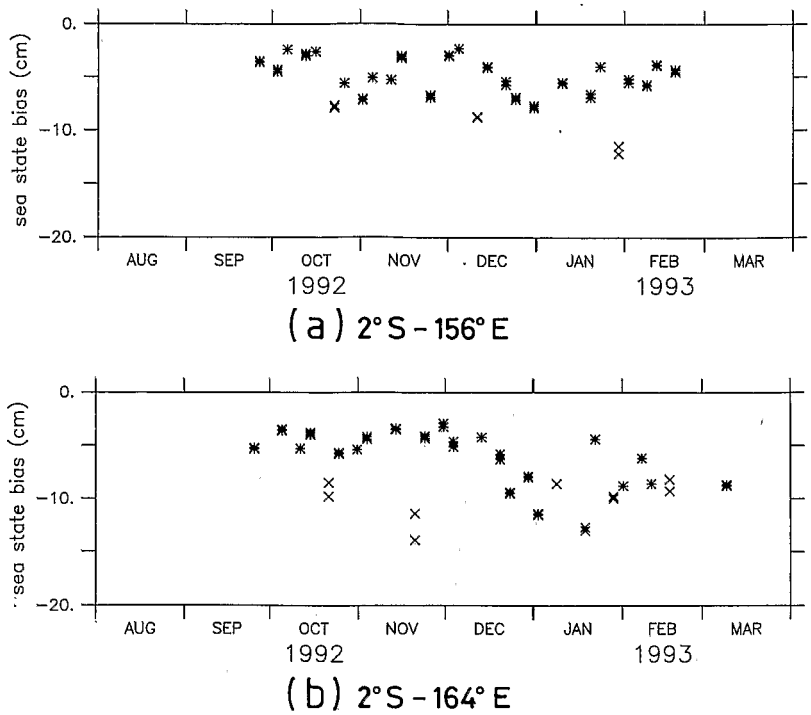

Figure 12. Sea state correction from the TOPEX (stars) and POSEIDON (crosses) altimeters at (a) 2°S-156°E and (b) 2°S-164.4°E.

surface dynamic height and TOPEX/POSEIDON sea level measurements falling in the 20° longitude by 10° latitude box. Figure 13 clearly shows the need of low-pass filtering for both series and especially for the TOPEX/POSEIDON sea level. With the 10-day repeat orbit one would not expect to study phenomena with period lower than the Nyquist 20-day period. In addition, the main objective of the TOPEX/POSEIDON mission is to determine geostrophic surface current, and in the equatorial region, geostrophy applies at least on the monthly timescale [*Picaut et al.*, 1989]. Therefore we have chosen a 30-day Hanning filter for the low-frequency comparison of the TOPEX/POSEIDON and surface dynamic height.

The TOPEX/POSEIDON data were also processed using two-dimensional (2-D) (x-y) and three-dimensional (3-D) (x-y-t) optimal interpolation techniques. The results for the 3-D optimal interpolation are presented in Figure 14. The decorrelation scales were chosen in space following *Meyers et al.* [1991], with 15° longitude and 3° latitude, and in time from the autocorrelation of the surface dynamic height time series at the two sites (25 days). We have tried to improve the low-frequency comparison by introducing a 2.6 m s^{-1} eastward phase propagation into the 3-D optimal interpolation scheme, assuming that the largest sea level variations at the mooring sites were associated with equatorial Kelvin wave propagation (section 3). As can be seen in Table 5, this technique only slightly improved the low-frequency comparison. Following the technique used by *Picaut et al.* [1990] for the determination of surface geostrophic currents at the equator from Geosat data, a combination of linear (Hanning) and nonlinear (median) filters was also used along each individual track in order to reduce possible remaining noise or spikes along the track (400-km filter length). Such filtering had a negligible impact on the comparison, consistent with the reduction in along-track noise in TOPEX/POSEIDON data compared with Geosat data.

Our ability to determine the appropriate technique is impacted by the relatively short duration of the times series, and it is not clear that the low-frequency comparison benefits from these additional techniques (2-D, 3-D, 3-D with propagation) beyond the comparison from the straightforward binning utilized at first (Table 5). Overall, the low-frequency comparison results in a very good correspondence between the TOPEX/POSEIDON sea level anomalies and the sea surface dynamic height anomalies, with correlation of 0.93–0.96 and rms difference of 1.6–2.0 cm. This result is particularly good, considering the low-frequency barotropic signal could not be determined from our observations.

5. Discussion and Conclusions

In the previous sections we have presented a comparison of TOPEX and POSEIDON altimeter data and in situ time series data from two heavily instrumented ATLAS moorings of the TOGA-TAO array in the western equatorial Pacific. The analysis was performed during the TOPEX/POSEIDON verification phase, spanning a 6–7 month period following the launch of the satellite. The period of our study also overlapped in time with the TOGA-COARE intensive observation period (November 1992 to February 1993), providing a valuable, regional-scale observational framework in which to interpret the variations observed in both the satellite and moored time series data.

For the purpose of TOPEX/POSEIDON validation, standard instrumentation on the two ATLAS moorings was augmented with temperature sensors over the full depth of the water column and, in the upper 750 m, with conductivity sensors (to estimate salinity) and pressure sensors. From these

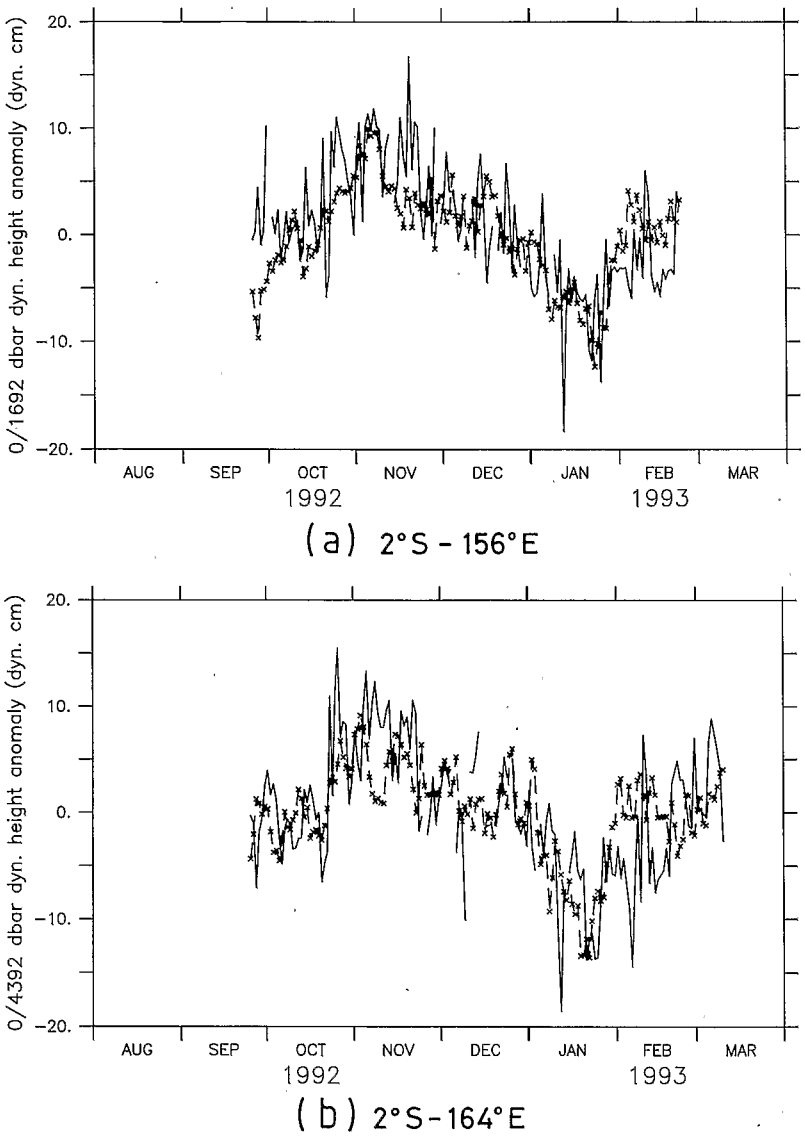

Figure 13. Comparison between the daily mean sea surface dynamic height (crosses) and the daily binned TOPEX/POSEIDON (solid lines) sea level within a 20° longitude × 10° latitude box at (a) 2°S-156°E and (b) 2°S-164.4°E.

data, surface dynamic heights relative to the bottom were computed with a temporal resolution of 5 min. We estimated the accuracy of our surface dynamic height calculation at 2°S-156°E to be roughly 1 dyn. cm. The accuracy at 2°S-164.4°E is probably closer to 1.5 dyn. cm because of the coarser vertical resolution of subsurface temperature and salinity, because of the imprecise determination of the vertical displacements of the sensors below 750 m, and because the range of depths over which density was integrated to provide dynamic height estimates was greater there. Bottom pressure gauges were also deployed near the two ATLAS moorings to estimate the barotropic component of sea level. One of these instruments failed after 21 days (at 2°S-156°E), and both were affected by a low-frequency drift. Hence use of these data was confined to analysis of the tides, which at the diurnal and semidiurnal frequencies are the most energetic components of barotropic sea level variability.

Both "instantaneous" and "low-frequency" comparisons were performed using the anomalies of in situ dynamic height estimates and of satellite altimeter data. Instantaneous comparisons were intended to assess the accuracy of the altimeters and of the various corrections, whereas the low-frequency comparisons were done to assess the potential reduction of sampling errors (primarily due to tidal aliasing) by temporally and spatially averaging. For the instantaneous comparisons a number of TOPEX/POSEIDON 1-s data points around the mooring sites were compared to the closest 5-min surface dynamic height estimates from the moorings. For the low- frequency comparisons we combined altimeter data around each validation site, either with a simple binning technique or with an optimal interpolation technique, then low pass filtered the time series with a 30-day Hanning filter length.

Instantaneous comparisons based on in situ dynamic height measurements and on altimeter retrievals corrected using the *Schwiderski* [1980] tidal model and ECMWF surface air pressure analyses to account for the inverted barometer effect indicate rms differences of 3.6 cm at 2°S-156°E and 4.4 cm at 2°S-164.4°E. Note that these rms differences are reduced by 0.5

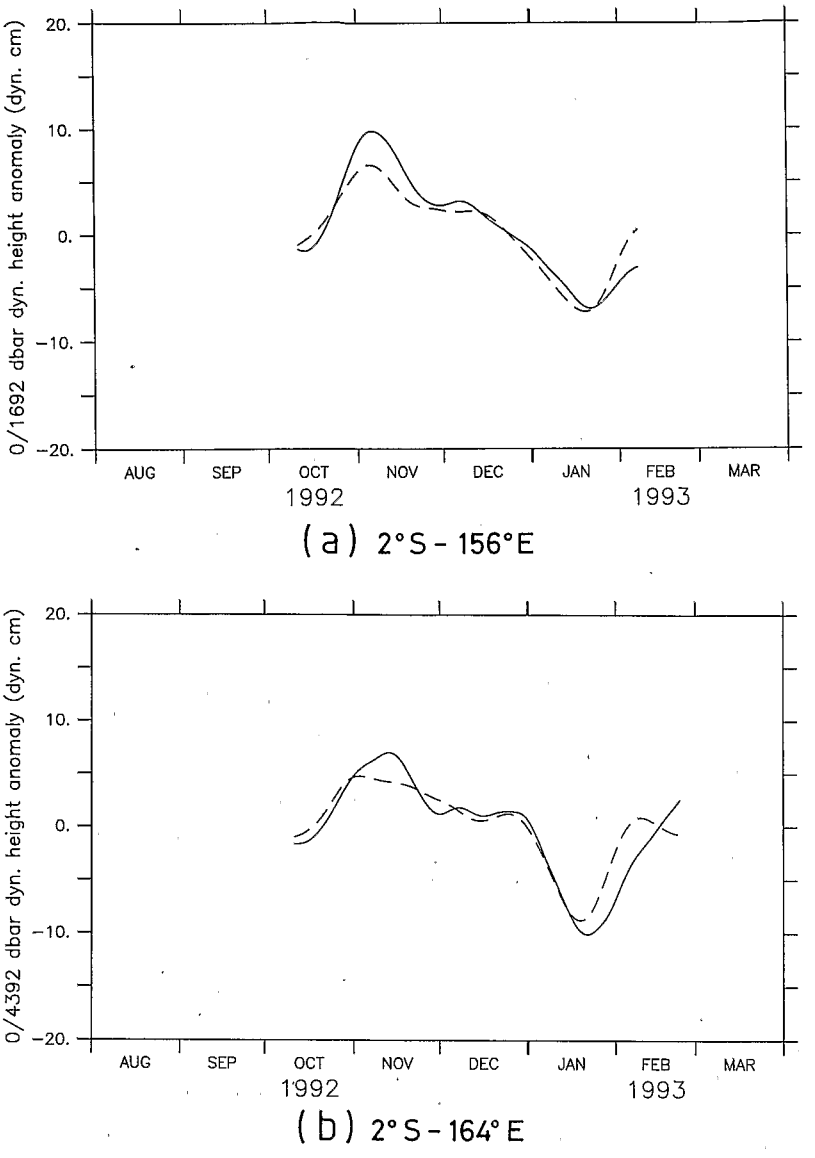

Figure 14. Low-frequency (30-day Hanning filter) comparison between the sea surface dynamic height (dashed lines) relative to bottom and the TOPEX/POSEIDON sea level from the three-dimensional optimal interpolation (solid lines) at (a) 2°S-156°E and (b) 2°S-164.4°E.

cm when POSEIDON data are omitted. With a 1- to 1.5-cm error in the dynamic height calculation at the mooring validation sites these results suggest an altimeter measurement error of 3–4 cm at the two locations. The actual error may be even smaller because our comparisons are not truly instantaneous, since the satellite and in situ measurements may be separated by up to 5 min in time and 6 km in space. Moreover, we have not been able to estimate low-frequency barotropic sea level variations from the BPR data because of sensor drift. This component of sea level variation, to the extent that it may be significant, is likewise included in the in situ/satellite differences.

The accuracy of the TOPEX/POSEIDON altimeter sea level measurements is sensitive to the choice of tidal correction scheme. Indeed, our low-frequency comparisons have been based on the tidal model correction [*Schwiderski*, 1980] that give, on a mean, the smallest rms instantaneous differences between the in situ and satellite measurements. For the three tidal models tested in this study the rms differences ranged from 3.6 to 4.6 cm at 2°S-156°E and from 4.1 to 4.6 cm at 2°S-164.4°E. We suspect, however, that the relative improvement in satellite sea level estimates based on different tidal models has a regional and temporal dependence. For example, *Busalacchi et al.* [1994] noted considerable improvement in the eastern equatorial Pacific using the tidal corrections of *Ray et al.* [1994]. Thus the results of our study should not be generalized to imply that the Schwiderski model is best for the purpose of correcting TOPEX/POSEIDON altimeter retrievals on a global basis at all times.

The rms difference between in situ dynamic height and instantaneous altimeter sea level decreased from 3.6 to 3.3 cm when substituting moored surface air pressure measurements for the ECMWF analyses at 2°S-156°E. From this small difference we would conclude that, at least at this location, the ECMWF surface pressure analysis provided a satisfactory correction for the inverted barometer effect. However, the air pressure variations were not particularly strong at the valida-

Table 5. Correlation and rms Difference Between Low-Frequency Sea Surface Dynamic Height and TOPEX/POSEIDON Sea Level Anomalies Using Different Space-Time Interpolation Schemes

	Longitude by Latitude, deg			Optimal Interpolation		
	20 × 10	10 × 3	5 × 2	2-D	3-D	3-D With Propagation
			2°S-156°E			
Correlation	0.96	0.96	0.97	0.96	0.96	0.96
rms difference	1.7	1.8	2.2	2.0	1.8	1.6
			2°S-164.4°E			
Correlation	0.89	0.95	0.97	0.94	0.94	0.93
rms difference	2.2	1.5	1.3	1.6	1.9	1.8

Units are centimeters.

tion mooring sites, with an observed 1.6-mbar standard deviation near 2°S-156°E. As with our conclusion regarding tidal models, it would be inappropriate to generalize about the suitability of the ECMWF pressure analyses to other times and other parts of the world ocean where air pressure variations may be much stronger than observed during the 6 months of our study, where the data density going into the ECMWF analysis scheme may vary, and where the ocean's response may be dynamically different.

One of the more striking phenomenon detected in our dynamic height time series was the quasi-permanence of semidiurnal internal tides, with an rms amplitude of 2.3 cm at 2°S-156°E and 1.4 cm at 2°S-164.4°E. It is commonly believed that internal tides are generated by scattering of the barotropic tides in regions of irregular bottom topography [e.g., *Hendershott*, 1981; *Morozov*, 1995]. Thus the higher internal tidal amplitudes at 2°S-156°E are probably induced by the Ontong Java Plateau, where the mooring was anchored in the proximity of rough topography with reefs, islands, and trenches. In contrast, the 2°S-164.4°E mooring was deployed in the Nauru Basin, an abyssal plain characterized by much smoother bottom topography, farther from potential source regions than the 2°S-156°E site.

Associated with the internal tides at 2°S-156°E, there were episodes of large-amplitude (up to 30 dyn. cm) dynamic height increases which occurred abruptly within the span of 1 hour. These episodes generally occurred once per semidiurnal tidal cycle and were usually clustered in groups extending over several days. It is likely that these large dynamic height changes at 2°S-156°E were a manifestation of solitary waves, generated in tandem with the internal tides in the region of rough bottom topography to the west and southwest of the mooring site. Similar abrupt dynamic height variations did not occur at 2°S-164.4°E over the abyssal plain, consistent with the hypothesis of generation by topographic scattering of barotropic tides.

Our observations suggest that the phase of the internal tides varied randomly relative to the barotropic tides, though their amplitude seemed sporadically related to the spring tides. Internal tides and dynamically related solitary waves in regions of rough topography are very difficult to predict. Therefore they are a source of sampling error in the determination of lower-frequency variations from altimeter records. For low baroclinic mode motions one expects the horizontal scale (1/4 wavelength) of internal tides to be about 20–30 km. Solitary waves observed near 2°S-156°E during COARE were coherent over similar distances along crest. For the instantaneous comparisons, best results (rms difference of 3–4 cm) were obtained by choosing only the four closest points in time and space to each 5-min dynamic height, i.e., within a maximum of 7 km from the mooring sites. This suggests that internal tides and solitons were seen, simultaneously in surface dynamic height and altimeter measurements, with similar amplitudes. Thus it should be possible to reduce the signature of the internal tides and other sources of short timescale and space-scale geophysical noise in altimeter analyses by implementing suitable space-time averaging schemes. Our low-frequency comparisons between in situ dynamic height estimates and TOPEX/POSEIDON retrievals indeed indicated a reduction in sampling errors when additional TOPEX/POSEIDON data are considered around the mooring sites. For example, by grouping the altimeter data in 10° longitude by 3° latitude boxes around the mooring sites and smoothing with 30-day Hanning filter, we found correlation greater than 0.95 and rms differences with the in situ data of less than 2 cm. However, increasing the size of the box does not systematically improve the low-frequency comparison, nor does the use of sophisticated optimum interpolation techniques.

In conclusion, our analysis suggests that the TOPEX/POSEIDON altimeter can provide instantaneous measurements of the sea surface dynamic topography accurate to 3–4 cm, depending on the choice of tidal correction scheme. This accuracy is remarkable, considering the complexity of the satellite sensor and tracking system and the data processing and correction schemes required to derive oceanographically relevant information. Moreover, it is worth noting that the low-frequency comparison succeeded in going below the 2-cm expected accuracy of the TOPEX/POSEIDON mission. Although based on only a limited amount of data in the western Pacific for a 6–7 month period, our results indicate that the TOPEX/POSEIDON data stream will prove to be an invaluable tool for seasonal to interannual climate studies in the tropical oceans, where sea level is both a proxy for upper ocean heat content and where geostrophic current variations are sensitive to small changes in sea level gradients.

Acknowledgments. The authors wish to thank a number of persons who made this validation experiment possible. Linda Mangum, Andy Sheperd, Francis Gallois, Jacques Grelet, and Gérard Eldin were of great help in the preparation of the equipment and in the operations at sea. Marie-Jo Langlade, Mary Eble, Margie McCarty, and Paul Freitag helped tremendously in the data preparation and analyses. Chet Koblinsky and Christian Le Provost kindly provided the improved TOPEX/POSEIDON GDR and the tidal constituents, respectively. Discussions with Harold Mofjeld, Richard Ray, Florent Lyard, Philippe Dandin, and Patrick Vincent helped in the interpretation of our results. Comments on a previous manuscript from Bob Cheney and an anonymous reviewer are appreciated. Roger Lukas and Bob Weller are greatly acknowledged for providing additional Seacat and sea level pressure data as part of NSF TOGA-COARE proposals. This validation experiment was made possible through the funding provided by NASA, CNES, NOAA, ORSTOM, and PNTS, and the efforts of Bill Patzert, Bob Cheney, and Alain Ratier in setting up these funds on short notice are greatly appreciated. JISAO contribution 333. PMEL contribution 1658.

References

Boss, E. F., and F. I. Gonzalez, Signal amplitude uncertainty of a Digiquartz pressure transducer due to static calibration error, *J. Atmos. Oceanic Technol.*, *11*, 1381–1387, 1994.

Boulanger, J.-P., and C. Menkes, Propagation and reflection of long equatorial waves in the Pacific Ocean during the 1992–1993 El Niño, *J. Geophys. Res.*, this issue.

Busalacchi, A. J., M. J. McPhaden, and J. Picaut, Variability in equatorial Pacific sea surface topography during the verification phase of the TOPEX/POSEIDON mission, *J. Geophys. Res.*, *99*, 24,725–24,738, 1994.

Cartwright, D. E., and R. D. Ray, Oceanic tides from Geosat altimetry, *J. Geophys. Res.*, *95*, 3069–3090, 1990.

Chapman, S., and R. S. Lindzen, *Atmospheric Tides: Thermal and Gravitational*, 200 pp., Gordon and Breach, New York, 1970.

Delcroix, T., G. Eldin, and C. Hénin, Upper ocean water masses and transports in the western tropical Pacific, *J. Phys. Oceanogr.*, *17*, 2248–2262, 1987.

Delcroix, T., J. Picaut, and G. Eldin, Equatorial Kelvin and Rossby waves evidenced in the Pacific Ocean through Geosat sea level and surface current anomalies, *J. Geophys. Res.*, *96*, 3249–3262, 1991.

Delcroix, T., J. P. Boulanger, F. Masia, and C. Menkes, Geosat-derived sea level and surface current anomalies in the equatorial Pacific during the 1986-1989 El Niño and La Niña, *J. Geophys. Res.*, *99*, 25,093–25,107, 1994.

Eble, M. C., and F. I. Gonzalez, Deep-ocean bottom pressure measurements in the Northeast Pacific, *J. Atmos. Oceanic Technol.*, *8*, 221–233, 1991.

Eldin, G., T. Delcroix, C. Hénin, K. Richards, Y. du Penhoat, J. Picaut, and P. Rual, Large-scale current and thermohaline structures along 156°E during the COARE Intensive Observation Period, *Geophys. Res. Lett.*, *21*, 2681–2684, 1994.

Fischer, M., M. Latif, M. Flügel, and J. Zou, Assimilation of sea level data into a primitive equation model, *TOGA Notes*, vol. *15*, pp. 1–5, Nova Southeast. Univ. Press, Dania, Fla., 1994.

Foreman, M. G. G., Manual for tidal heights analysis and prediction, *Pac. Mar. Sci. Rep. 77-10*, 70 pp., Inst. of Ocean Sci., Patricia Bay, Victoria, B. C., 1977.

Fu, L. L., and G. Pihos, Determining the response of sea level to atmospheric pressure forcing using TOPEX/POSEIDON data, *J. Geophys. Res.*, *99*, 24,633–24,642, 1994.

Gaspar, P., F. Ogor, P.-Y. Le Traon, and O.-Z. Zanife, Estimating the sea state bias of the TOPEX and POSEIDON altimeters from crossover differences, *J. Geophys. Res.*, *99*, 24,981–24,994, 1994.

Gourdeau, L., J. Picaut, M.-J. Langlade, A. J. Busalacchi, E. Hackert, M. J. McPhaden, H. P. Freitag, F. I. Gonzalez, M. C. Eble, and R. A. Weller, Data preparation for the open-ocean validation of TOPEX/POSEIDON sea level in the western equatorial Pacific, *Rapp. Sci. Tech., Sci. Mer, Oceanogr. Phys.*, ORSTOM, Nouméa, New Caledonia, in press, 1995.

Hayes, S. P., L. J. Mangum, J. Picaut, A. Sumi, and K. Takeuchi, TOGA-TAO: A moored array for real-time measurements in the tropical Pacific Ocean, *Bull. Am. Meteorol. Soc.*, *72*, 339–347, 1991.

Hendershott, M. C., Long waves and ocean tides, in *Evolution of Physical Oceanography*, edited by B. A. Warren and C. Wunsch, pp. 292–341, MIT Press, Cambridge, Mass., 1981.

Katz, E. J., A. Busalacchi, M. Bushnell, F. Gonzalez, L. Gourdeau, M. McPhaden, and J. Picaut, A comparison of coincidental time series of the ocean surface height by satellite altimeter, mooring, and inverted echo sounder, *J. Geophys. Res.*, this issue.

Kessler, W. S., and M. J. McPhaden, Equatorial waves and the dynamics of the 1991–93 El Niño, *J. Clim.*, in press, 1995.

Kessler, W. S., M. J. McPhaden, and K. M. Weickmann, Forcing of intraseasonal Kelvin waves in the equatorial Pacific, *J. Geophys. Res.*, *100*, 10,613–10,631, 1995.

Le Provost, C., A. F. Bennett, and D. E. Cartwright, Ocean tides for and from TOPEX/POSEIDON, *Science*, *267*, 639–642, 1995.

Madden, R. A., and P. R. Julian, Detection of a 40–50 day period oscillation in the zonal wind in the tropical Pacific, *J. Atmos. Sci.*, *28*, 702–708, 1971.

McPhaden, M. J., TOGA-TAO and the 1991–93 El Niño-Southern Oscillation event, *Oceanography*, *6*, 36–44, 1993.

McPhaden, M. J., A. J. Busalacchi, and J. Picaut, Observations and wind-forced model simulations of the mean seasonal cycle in tropical Pacific sea surface topography, *J. Geophys. Res.*, *93*, 8131–8146, 1988.

Ménard, Y., E. Jeansou, and P. Vincent, Calibration of the TOPEX/POSEIDON altimeters at Lampedusa: Additional results at Harvest, *J. Geophys. Res.*, *99*, 24,487–24,504, 1994.

Menkes, C., J.-P. Boulanger, and A. J. Busalacchi, Evaluation of TOPEX and basin-wide TOGA-TAO sea surface topographies and derived geostrophic currents, *J. Geophys. Res.*, this issue.

Meyers, G., H. Philips, N. Smith, and J. Sprintall, Space and time scales for optimal interpolation of temperature tropical Pacific Ocean, *Prog. Oceanogr.*, *28*, 189–218, 1991.

Miller, A. J., L. D. S. Luther, and M. C. Hendershott, The fortnightly and monthly tides: Resonant Rossby waves or nearly equilibrium gravity waves?, *J. Phys. Oceanogr.*, *23*, 879–897, 1993.

Miller, L., R. E. Cheney, and B. C. Douglas, GEOSAT altimeter observations of Kelvin waves and the 1986–87 El Niño, *Science*, *239*, 52–54, 1988.

Mofjeld, H. O., F. I. Gonzalez, M. C. Eble, and J. C. Newman, Ocean tides in the continental margin off the Pacific northwest shelf, *J. Geophys. Res.*, *100*, 10,789–10,800, 1995.

Morozov, E. G., Semidiurnal internal wave global field, *Deep Sea Res., Part I*, *42*, 135–148, 1995.

Nerem, R. S., E. J. Schrama, C. J. Koblinsky, and B. D. Beckley, A preliminary evaluation of ocean topography from the TOPEX/POSEIDON mission, *J. Geophys. Res.*, *99*, 24,565–24,583, 1994.

Picaut, J., and T. Delcroix, Equatorial wave sequence associated with warm pool displacements during the 1986–1989 El Niño-La Niña, *J. Geophys. Res.*, *100*, 18,393–18,408, 1995.

Picaut, J., M. J. McPhaden, and S. P. Hayes, On the use of the geostrophic approximation to estimate time-varying zonal currents at the equator, *J. Geophys. Res.*, *94*, 3228–3236, 1989.

Picaut, J., A. J. Busalacchi, M. J. McPhaden, and B. Camusat, Validation of the geostrophic method for estimating zonal currents at the equator from Geosat altimeter data, *J. Geophys. Res.*, *95*, 3015–3024, 1990.

Ponte, R. M., D. A. Salstein, and R. D. Rosen, Sea level response to pressure forcing in a barotropic numerical model, *J. Phys. Oceanogr.*, *21*, 1043–1057, 1991.

Ray, R. D., B. V. Sanchez, and D. E. Cartwright, Some extensions to the response method of tidal analysis applied to TOPEX/POSEIDON altimetry, *Eos Trans. AGU*, *75*(16), Spring Meet. suppl., 108, 1994.

Schwiderski, E. W., On charting global ocean tides, *Rev. Geophys.*, *18*, 243–268, 1980.

TOPEX/POSEIDON Joint Verification Team, TOPEX/POSEIDON joint verification plan, *JPL Publ.*, *92-9*, 92 pp., 1992.

TOPEX/POSEIDON Science Working Team, TOPEX/POSEIDON Science Investigations Plan II, The mission, *JPL Publ.*, *91-27*, 7–15, 1991.

Watts, R. D., and H. Kontoyiannis, Deep-ocean bottom pressure measurement: Drift removal and performance, *J. Atmos. Oceanic Technol.*, *7*, 296–306, 1990.

Webster, P. J., and R. Lukas, TOGA-COARE: The coupled ocean-atmosphere response experiment, *Bull. Am. Meteorol. Soc.*, *73*, 1377–1416, 1992.

Wunsch, C., The long-period tides, *Rev. Geophys.*, *5*, 447–475, 1967.

A. J. Busalacchi, Laboratory for Hydrospheric Processes, NASA Goddard Space Flight Center, Code 970, Greenbelt, MD 20771.

F. I. Gonzalez and M. J. McPhaden, Pacific Marine Environmental Laboratory, NOAA, 7600 Sand Point Way, NE, Seattle, WA 98115.

L. Gourdeau and J. Picaut, Groupe SURTROPAC, l'Institut Français de Recherche Scientifique pour le Développement en Coopération (ORSTOM), BP 5, Nouméa, New Caledonia. (e-mail: picaut@noumea.orstom.nc)

E. C. Hackert, Laboratory for Hydrospheric Processes, NASA Goddard Space Flight Center, Hughes STX Corporation, Code 970, Greenbelt, MD 20771.

(Received February 6, 1995; revised July 11, 1995;
accepted July 11, 1995.)